UiT The Arctic University of Norway

Faculty of Science and Technology
Department of Engineering and Safety

A Feasibility Study of Using Waste Thermal Energy from a District Heating System for Absorption Cooling

Gerald Nsenkeng Obi

TEK-3901 Master's thesis in Technology and Safety in the High North
July 2020

Study: **TEK-3901 Technology and Safety in the High North**	Academic Year: **2020**

Title: **A Feasibility Study of Using Waste Thermal Energy from a District Heating System for Absorption Cooling**	Date: **13.07.20** Grading: **Open** Number of pages: **81** Number of appendices: **5** Confidentiality: **None**
Author: **Gerald Nsenkeng Obi**	
Supervisors: **Jinmei Lu, Professor Javad Barabady**	
Contracting Authority: **UIT, The Arctic University of Norway**	Contracting Authority Supervisor: **Jinmei Lu, Professor Javad Barabady, UIT**

Summary: The waste incineration industry in Norway has seen a massive growth since its large-scale implementation. The thermal energy recovered from waste incineration in Norway is mainly used in power production and district heating. However, with increasingly warmer summer months due to climate change, several plants struggle with energy efficiency during this period due to low heating demand, which results in thermal energy waste to ambient air. The release of waste energy is costly and not energy efficient. Therefore, it is of great importance to find economically and environmentally friendly solutions for this waste energy. This study aims at presenting an overview of the waste incineration industry in Norway and the current options for surplus energy from waste incineration. Additionally, the aim is to analyze and identify the energy efficiency difficulties in the current system of a selected waste incineration plant and propose a more energy efficient alternative system. In this study, Returkraft AS, Kristiansand, Norway is selected as the case study. Data obtained from the plant is analyzed to propose an alternative system which can easily be integrated into the existing setup of the plant. An absorption chiller model is built on ASPEN PLUS to simulate the amount of cooling which could be achieved with the recovered waste heat. MATLAB is used to simulate the heat transfer across the fluids to determine the required heat transfer area for the heat exchangers in the proposed system. An economic evaluation is carried out to estimate the investment cost and payback time of the proposed system. Additionally, a brief environmental analysis is performed, presenting the environmental impacts of the proposed system. The results presented show that up to 2.33 MW of absorption cooling can be achieved supplying chill water at 7.01°C with a COP of 0.72, and the proposed system can improve the energy utilization of the plant during the warmer months of May – September from 41% to about 95%. The estimated payback times were 1.3 and 1.5 years for two income stream scenarios, which could be considerably higher than estimated depending on a range of factors. Nonetheless, the proposed system provides substantial thermal energy saving potentials with significant energy efficiency and environmental benefits.

Keywords: Waste Incineration, District Heating, Waste Heat, Absorption Cooling, Heat Exchanger, Thermal Energy

Abstract

Waste incineration-based district heating plants in Norway struggle from energy efficiency drawbacks during the warmer months of the year from May - September due to the reduced demand in heating.

As a result, thermal energy gets discarded to ambient air, which affects the energy efficiency of the plants. This study aims at presenting an overview of the waste incineration industry in Norway and the current options for surplus energy from waste incineration. Additionally, the aim is to analyze and identify the energy efficiency difficulties in the current system of a selected waste incineration plant and propose a more energy efficient alternative system. A waste incineration plant Returkraft AS in Kristiansand, located in southern Norway is selected as a case study and the thermal energy production process in this plant is analyzed.

The analysis of Returkraft´s production data revealed that averagely 10 836 MWh of thermal energy gets discarded monthly to ambient air during the warmer months. An alternative system where the otherwise wasted thermal energy is used in absorption cooling is put forward, and simulations are carried out on ASPEN PLUS to present how much cooling can be achieved with the available waste heat.

The results indicate that up to 2.33 MW of cooling can be achieved, producing chilled water at a temperature of 7.01°C. A COP of 0.72 was achieved which is above the average COP of a single effect commercial absorption chiller. The results further present the energy utilization improvement from 41% with the current system to 95% with the proposed system during the warmer months.

Despite investment costs being high with a possibly lengthy payback time, waste incineration plants in Norway are encouraged nonetheless to make energy efficiency improvements to their plants. The massive benefits of waste heat recovery with a wide range of applications available make the investments worthwhile long-term.

Preface and Acknowledgement

This study is the last part of a two-year master program in Technology and Safety in the High North at UIT- The Arctic University of Norway, Department of Engineering and Safety and constitutes 30 ECTS credits. It is an independent work prepared by me, Gerald Nsenkeng Obi between January 2020 and July 2020. This study contains about 19 150 words, 12 tables and 27 figures.

This study is aimed at students, engineers and interested persons with a technical understanding and background. The literature and technical formulas in the study are comprehensive and presented in a simple manner, but some basic knowledge about process engineering and mathematics is required in order to get familiar with the study.

Numerous persons deserve my appreciation and I am grateful for their contribution to this study. Firstly, I would like to express my heartfelt gratitude to my supervisors Associate Professor Jinmei Lu and Professor Javad Barabady from the Department of Technology and Safety of UIT- The Arctic University of Norway for guidance and input on this study. I would like to thank Doctoral Research Fellow Steve Jackson from the Department of Automation and Process Engineering at UIT- The Arctic University of Norway for assistance with the ASPEN PLUS license and installation which was vital in completing this study.

I would also like to thank Jostein Mosby, head of strategic maintenance at Returkraft AS, who was patient and always found time to provide me with data, clarifications and adequate explanations to my questions related to the plant.

I would like to acknowledge Trine Fjeldstad, senior consultant at the Norwegian Water Resources and Energy Directorate (NVE) who was helpful with data relevant to completing this study.

Finally, I would like to show profound gratitude to my family, especially my mom Noeline Goos, and my wife Jemea Limunga whose endless support and love gave me the courage to pursue my passion for engineering.

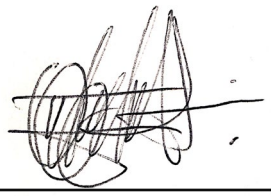

Gerald Nsenkeng Obi
Tromsø, July 2020

Table of Contents

List of Tables

List of Figures

List of Abbreviations

Acronym	Description
GWh/year	Giga Watt hour per year
W	Watt
kW	Kilowatt
kPa	Kilo Pascal
J	Joules
KJ	Kilojoules
Kg	Kilogram
s	Seconds
h	Hour
m	Meter
m^2	Square meter
Km	Kilometer
WtE	Waste to Energy
DCU	District Cooling Unit
AHU	Air Handling Unit
RO	Reverse Osmosis
SCR	Selective Catalytic Reduction
SNCR	Selective Non-Catalytic Reduction
SO_2	Sulfur dioxide

HCl	Hydrochloric acid
pH	Power of hydrogen
NO_X	Nitrogen oxides
NO	Nitric oxide
NO_2	Nitrogen dioxide
N_2	Nitrogen
H_2O	Water
NH_3	Ammonia
LiBr	Lithium bromide

1 Introduction

1.1 Background and problem statement

The waste management systems in Norway went through a change in 2009 after landfilling of biodegradable waste was forbidden, only hazardous waste could be disposed of in landfills [1]. Waste sorting instead was promoted for; food remains, paper, cartons, plastics, and Municipal Solid Waste (MSW) being waste which can´t be recycled. Presently, food remains are recycled for biogas and bio fertilizer production, paper, cartons and plastics are recycled to reproduce products which require the use of these materials, while MSW gets transported for waste incineration.

Waste incineration is the process of direct controlled burning of waste in the presence of oxygen at temperatures of about 800°C and above, liberating thermal energy, gases and inert ash. In practice, about 65 to 85% of the energy content of the organic matter can be recovered as heat energy, which can be utilized either for direct thermal applications such as; heating of buildings, or for producing power with the help of steam turbine-generators [2].

Waste incineration plants in Norway go back to 1967 with the construction of the Haraldrud plant which was the first large waste incineration plant in the country [3]. The incineration of waste is a better waste management method, since it can reduce pollution from the landfilling of waste.

Global mean temperatures have increased since the late 19th century [4]. The warming has been accompanied by an increase in extreme warm temperatures [5] and an increase in the occurrences of hot days [6].

For the period 1900-2008 as a whole, the annual mean temperature in Norway has increased by about 0.9°C. Depending on geographical region, the increase in annual temperature varies from 0.5 to 1.1°C [7]. Predicted changes from the current climate (baseline 1961 -1990) to the period 2071-2100 are that maximum temperatures in the summer will increase most in the south-east, with 3°C and about 2°C in the rest of the country [8].

This increase in average temperatures is being increasingly felt in Norway affecting thermal comfort in homes during the summer and early weeks of the autumn. This has led to a decrease in heating demand from waste incineration plants producing district heating during these seasons.

In the event of low heating demand during the summer and autumn seasons, less energy is recovered by client buildings resulting in the energy being rejected to ambient air. This is a waste of useful energy which could otherwise be recovered and used for applications such as; district cooling with absorption technology, storage for peak load heating in the winter, industrial process heating, or electricity generation with heat engines.

Several studies have been done in the past decade regarding the recovery of waste heat from various processes for different applications. M. Shakerin performed an analysis for using waste heat from cooling data centers and server aisles for district heating in Trondheim [9]. J. Wang & X. Gao studied the waste heat recovery from cooling water in chemical plants for building heating and cooling using a water source heat pump system and lithium bromide (LiBr) absorption heat pump system [10]. D.F Dominkovic explored the utilization of excess waste heat from natural gas power plants, Petro-chemical and waste incineration industries in hot climates with large cooling demands to produce cooling via absorption chillers [11]. S. Maurya, & D. Patel studied the recovery of waste heat from thermal power plants for cooling using combined vapor compression and vapor absorption refrigeration systems [12]. C.Y. Hsu et al studied waste heat recovery from a diesel power plant on Green Island for cooling using an absorption chiller [13].

However, none of these studies include the recovery of waste thermal energy from an existing district heating plant with low energy efficiency in the warmer months for cooling purposes, and no similar study has been done for Norway.

If the waste thermal energy recovered from existing district heating systems in waste incineration plants in Norway were to be used to produce cooling, the energy efficiency of the plants will be improved, better thermal comfort in homes during the summer and autumn seasons will be obtained, consequently reducing the load which individual electric cooling units would otherwise inflict on the electrical grid.

1.2 Research questions

In order to get to the point on how to make better use of the energy recovered from the existing waste incineration plants in Norway, it is important to first get an overview of the waste incineration industry in Norway and the current options for surplus energy from waste incineration. In this study, a waste incineration plant Returkraft AS in Kristiansand, located in southern Norway is selected as a case study. The thermal energy production process in this plant will be analyzed and the current application of the thermal energy will be explored. A picture of the surplus energy will be drafted and alternative applications of the excess energy will be put forward. Finally, an alternative system where the otherwise wasted thermal energy is put to useful service will be proposed.

The study results will answer the following research questions:

1. Which waste incineration plants are currently in operation in Norway? How much thermal energy is used and how much is wasted?
2. How is thermal energy produced from waste incineration and what are the main components of this process?
3. What are the current uses of the produced thermal energy at Returkraft AS?
4. What alternative system is recommended to better exploit the wasted excess resource and how can it be implemented?
5. Is it cost beneficial to implement the alternative system?
6. What are the environmental impacts of the alternative system?

1.3 Objective of the research study

The main objective of this study is to review the present state of the waste incineration industry in Norway and its efficiency and propose a more energy efficient system for better use of the produced thermal energy. The specific objectives of this research are to:

- Get an overview of the waste incineration industry in Norway.
- Understand the main components of the waste incineration process and get an overview of the thermal energy produced from waste incineration.
- Present the and analyze the current use of the produced thermal energy in Returkraft AS and understand the process of the surplus energy being put to waste.
- Explore an alternative system that can better use the wasted thermal energy.
    - Explain the process of district cooling and its main components.

    - Present how Returkraft AS could incorporate district cooling in its existing plant as a solution to reduce thermal energy waste.
    - Simulate the cooling production process to see the amount of cooling that can be achieved with the available waste heat.
- See if the alternative system is beneficial from an economical point of view using a cost-benefit analysis.
- Investigate if the alternative system is beneficial from an environmental point of view.

1.4 Limitation and challenges

This study only considers waste incineration within the waste to energy sector. Moreover, only the waste incineration plants currently operational in Norway are being introduced, providing an overview of their year of construction, year of upgrade, yearly waste burn, thermal energy production and use.

Within Norway, only one waste incineration plant is used as a case study to analyze the production data and identify drawbacks in potential efficiency with room for improvement. The plant´s monthly production data from the past 8 years was made available, but only data from the past three years was utilized due to limitation in time and for the simplicity of the study.

Due to the lack of some data, and the availability of data in ranges, reasonable estimates were made for the missing data and average values were used in order to complete the analyses. This will lead to insecurity of the analysis results.

Due to the COVID -19 outbreak and the travel restrictions, it was not possible to visit Returkraft´s plant and collect some data necessary for this study. Moreover, with the University campus closed during the quarantine period, it was not possible to carry-out the ASPEN PLUS simulations which required access to the campus PC-lab. Technical help was not available either for installation on a private PC. This considerably delayed the progress of this study.

1.5 Structure of the report

This study is structured as follows:

Chapter 1- Introduction: This chapter gives a background of the study, problems and challenges for the thermal energy from waste incineration plants, the research questions this study aims to answer and the objectives the study aims to research.

Chapter 2- Waste incineration in Norway & relevant theory: In this chapter, an introduction to the waste incineration industry in Norway is presented. The relevant theory of the waste incineration and thermal energy production process for electricity and district heating is also presented. Moreover, the relevant theory on the district cooling production process is shown in this chapter.

Chapter 3- Research methodology: In this chapter, the methodology that are used in this study are described in detail.

Chapter 4- Case study: The case study of this research is presented, as well as the issue in question which the study attempts to resolve.

Chapter 5- Results and discussion: In this chapter, the results from the study is presented and a discussion of the results is conducted.

Chapter 6- Conclusion: The conclusion of this study is presented in this chapter whereby relevant results are highlighted and discussed on how they tie to my hypothesis.

Chapter 7: Recommendations for future work: Some work which could be implemented in the future to provide continuance to this research study is presented in this chapter.

Chapter 8: References: It presents all the citations and references used in this study.

Chapter 9: Appendices: In this chapter, supplementary material to this study is presented.

2 Waste incineration in Norway & relevant theory

This chapter provides a brief introduction to the waste incineration industry in Norway, the relevant theory necessary for a better understanding of the research problem and proposed system.

2.1 Introduction to the waste incineration industry in Norway

In the late 1800s to early 1900s, waste in the city of Oslo was dumped on an island in the fjord. This method over time, led to poor air quality in the city of Oslo which made alternatives such as waste incineration more popular [14]. The Haraldrud plant was the first large waste incineration plant in Norway. It came into use in 1967 in Oslo and processed about 100 000 tons of household and commercial waste in a year. The plant produces energy in the form of warm water which is being distributed through a district heating network of underground pipes to Groruddalen in the north-east part of Oslo and Oslo city center [15].

There were several waste incineration plants across Norway after 1967. In 1981 the parliament approved a pollution control act, which aimed to protect the environment from pollution and reduce the amount of waste and promote better waste management [16]. This was due to the environmental problem of pollution gases which were being released to the environment during the waste incineration process. As a result of the stricter environmental requirements, the amount of waste incineration plants in Norway were reduced from 48 in 1989 to about 20 in 2019 [17]. While many plants closed down, a number of new plants that are more environmentally friendly were opened within that period. Some also upgraded their exhaust gas treating technologies and expanded the plant capacity for increased production. After compiling information available from the various plants´ webpages [18-34], it was established that presently there are 19 waste incineration plants still in operation across Norway. Table 1 is a list of the current operational plants from the oldest-serving to the youngest-serving plant.

Table 1. Overview of Waste Incineration Plants across Norway Currently in Operation

No	Plant	Location	Year of Construction/ Upgrade	Capacity	Recovered energy	Owner
1	Fortum Haraldrud	Haraldrud, Oslo	1967/ 2002	40 000 tons/year	District Heating 130 GWh/year	Fortum, Oslo municipality
2	Statkraft	Heimdal, Trondheim	1982/ 2007	200 000 tons/year	District heating 668,07 GWh/year	Statkraft
3	Senja Avfall IKS	Botnhågen, Finnsnes	1982/ 2007	11 000 tons/year	District heating 28,2 GWh/year, Electricity 1,8 GWh/year	6 municipalities in Troms
4	Fortum Klemetsrud	Klemetsrud, Oslo	1983/ 2011	375 000 tons/year	District heating 700 GWh/year, electricity 150 GWh/year	Fortum, Oslo municipality
5	Frevar	Øra, Fredrikstad	1984	92 000 tons/year	Steam 210 GWh/year	Frevar KF
6	Hallingdal Renovasjon IKS	Kleivi, Ål	1984	27 600 tons/year	District heating 28 GWh	6 municipalities in Hallingdal
7	Tafjord	Grautneset, Ålesund	1987/ 2009	100 000 tons/year	District heating 225 GWh/year & Electricity 25 GWh/year	Tafjord Kraft
8	Geithus forbrenningsanlegg	Geithus, Årdal	1994	2500 tons/year	Heating in the plant	Årdal municipality

9	BIR	Rådalen, Bergen	1999/ 2010	220 000 tons/year	District heating 270 GWh/year, Electricity 90GWh/year	Askøy, Bergen, Bjørnafjorden, Kvam, Osterøy, Samnanger og Vaksdal municipalities
10	Østfold Energi	Borregaard, Sapsborg	2002	75 000 tons/year	Steam 185 GWh/year	Østfold county municipality, 13 municipalities in Sapsborg
11	Forus	Stokka, Stavanger	2002/ 2013	110 000 tons/year	District heating 225 GWh/year, electricity 50 GWh/year	IVAR IKS, Lyse Neo AS, Westco AS
12	Østfold Energi	Mjørud, Rakkestad	2005	10 000 tons/year	Steam 22 GWh/year & district heating 3 GWh/year	Østfold county municipality, 13 municipalities in Sapsborg
13	Kvitebjørn Bio-El AS	Øra, Fredrikstad	2008	60 000 tons/year	Steam, District heating, electricity 160 GWh/year	Kvitebjørn Energi AS
14	Norcem Breivik	Breivik, Telemark	2009	50 000 tons/year	Process heating	Norcem
15	Norcem Kjøpsvik	Kjøpsvik, Narvik	2009	10 000 tons/year	Process heating	Norcem
16	Returkfraft	Langemyr, Kristiansand	2010	130 000 tons/year	District heating 250 GWh/year, electricity 95 GWh/year	21 municipalities in Adger

17	Hafslund Miljøenergi - Borregaard Waste to Energy	Borregaard, Sapsborg	2010	85 000 tons/year	Steam 230 GWh/year	Hafslund
18	Eidvisa Bioenergi	Trehørningen, Hamar	2011	78 000 tons/year	District heating 100 GWh/year, steam 50 GWh/year, electricity 50 GWh/year	Eidvisa Energi AS
19	Kvitebjørn Varme	Skattøra, Tromsø	2017	56 000 tons/year	District heating 126 GWh/year	Kvitebjørn Energi AS, Whitehelm Capital

2.2 District heating production process

The district heating production process takes several stages to achieve its output. The main processes are described below.

2.2.1 Water treatment

Water is a very important resource in the district heating production process because it is the medium that is used to recover the energy resulting from the incineration of waste. If the water supplied to the plant by the local municipality were to be pumped directly to the incinerator with high operating temperatures (800°C -1000°C) without passing through a water treatment process first, this could cause blockages and corrosion in pipes and equipment, thereby making the water treatment process vital. The water treatment is carried out through the process of reverse osmosis (RO). In this process the dissolved solids, color, organic contaminants and nitrate in the water are removed [35].

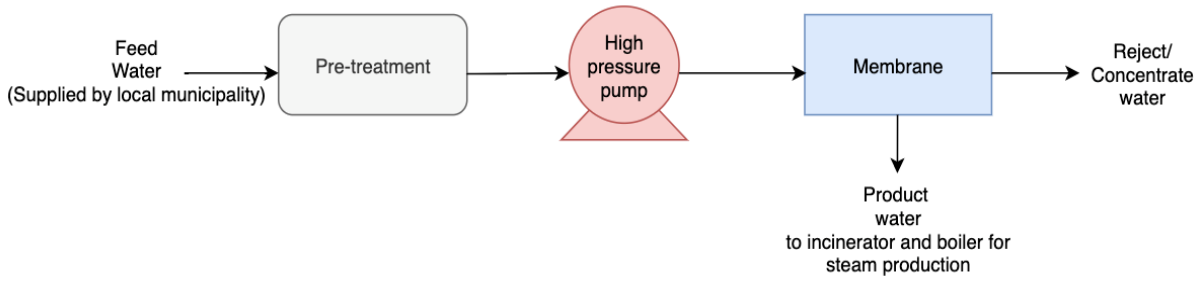

Figure 1. Simplified block flow of the Reverse Osmosis Process

A RO process consists of four main systems: Pre-treatment, High pressure pumps, Membrane, and Post-treatment. The raw water (feed water) normally supplied by the local municipality is fed to the pre-treatment system. This system is used to remove all solids and other contaminants from the water in order to avoid salt precipitation or microbial growth on the membranes. This system may involve chemical treatment followed by coagulation/flocculation/sedimentation, and sand filtration. The high-pressure pump system is used to provide the necessary pressure for the water which enables contaminants such as, salt to be removed from the water when passing through the membrane. The membrane system consists of a pressure vessel and a semi-permeable membrane inside which permits the feed water to pass through it and removes ions and unwanted molecules. Depending on the quality of water leaving the membrane and the use of the water; post treatment may consist of adjusting the pH level of the water and disinfection before the water is used in a process [35].

2.2.2 Waste feeder

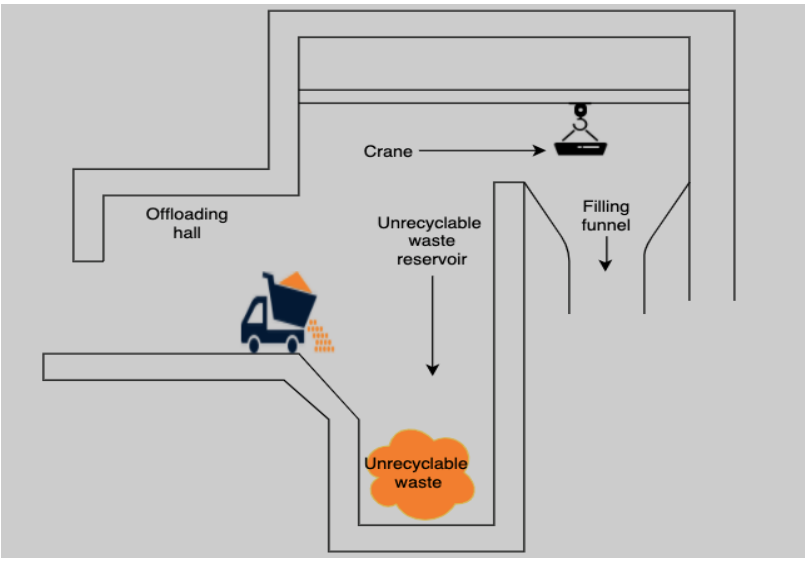

Figure 2. Waste feeder schematic

Unrecyclable waste is delivered to the plant offloading hall by container trucks where the waste is deposited into the waste reservoir. A crane operated both manually and automatically carries the waste from the waste reservoir constantly, and releases it into the filling funnel of the waste incinerator as illustrated in Figure 2. These reservoirs can store several tons of unrecyclable waste. As the crane operation attempts to empty the reservoirs, more waste is delivered to the plant which results in huge amounts of unrecyclable waste always being available in the reservoirs.

2.2.3 Incinerator and energy recovery

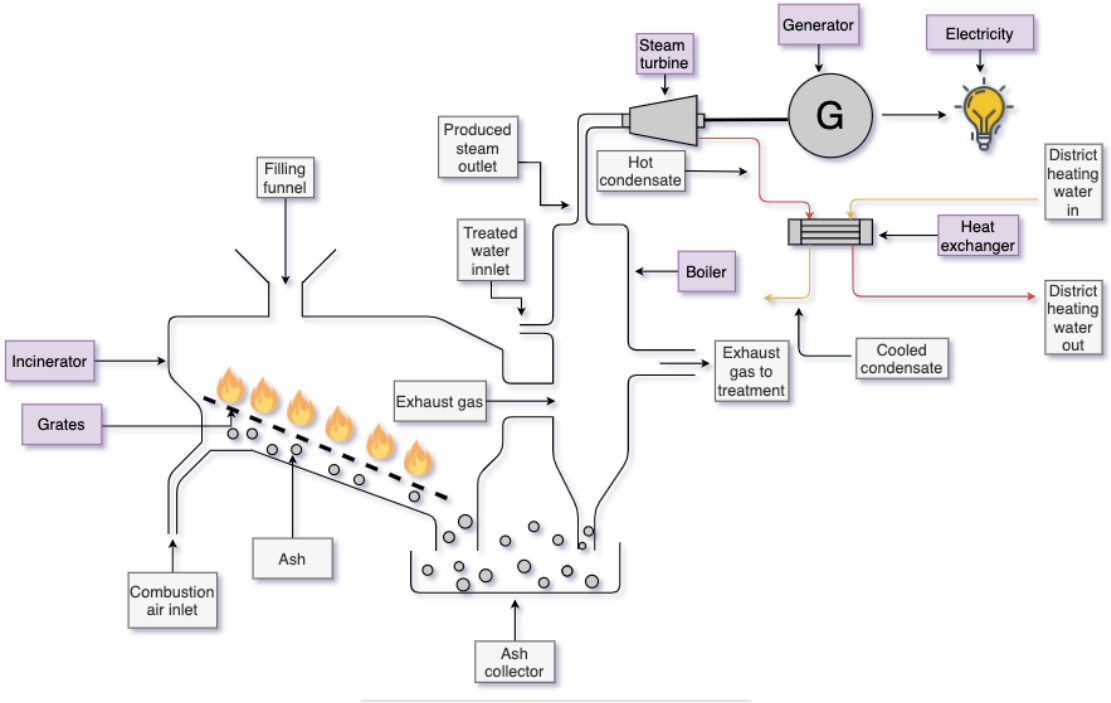

Figure 3. Waste incineration and energy recovery schematic

When the waste is transported into the filling funnel, it ends up on the incineration grates of the waste incinerator. The waste is incinerated on the grates and the ashes fall to the bottom through the grates. The ashes are collected into the ash collector before being transported for use in asphalt mixtures for the construction of roads, for use in cement production or to landfills. The extremely hot exhaust gases travel into the boiler where the energy from the gases are transferred to the treated water in the boiler, converting it into superheated steam. This steam leaves the boiler and is used to drive a steam turbine which is connected to a generator that in turn produces electrical energy. After transferring its energy, the steam condenses into hot condensate which leaves the steam turbine and is transported by pumps into one end of a heat exchanger. The heat exchanger on the other end is connected to a closed water cycle where the

water is heated by the hot condensate, recovering the energy from the condensate. The hot condensate leaves the heat exchanger as cool condensate, while the cool water entering the heat exchanger leaves at a considerably higher temperature. This hot water is then used to heat up buildings by means of a district heating network of underground pipes and heat exchangers installed in these buildings. The cool condensate on the other hand is re-sent into the boiler to recover more energy from the hot exhaust gas and the process repeats itself. In certain plants that do not produce electricity, the hot steam from the boiler is sent directly into a heat exchanger where the energy is transferred to the water in a closed water cycle for district heating purposes.

The exhaust gas from the boiler is then sent to a gas treatment process for further treatment.

2.2.4 Gas treatment

The gas treatment is an important process to reduce the pollutant in the gas to acceptable levels according to air quality standards. There are normally two exhaust gas treatment stages in a waste incineration plant i.e. the primary gas treatment, and the secondary gas treatment.

2.2.4.1 Primary gas treatment

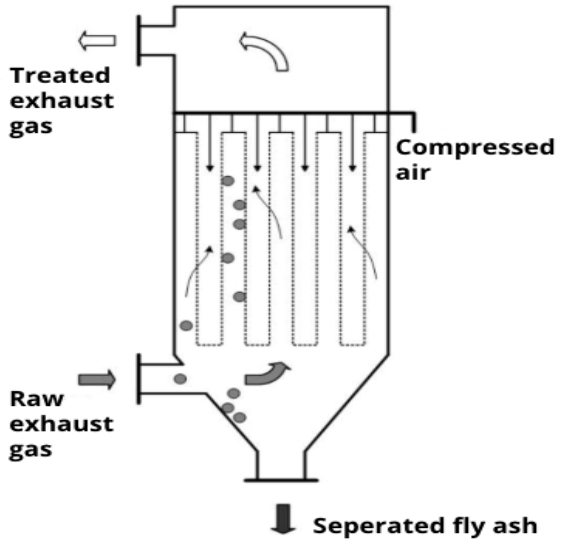

Figure 4. Bag filter components [36]

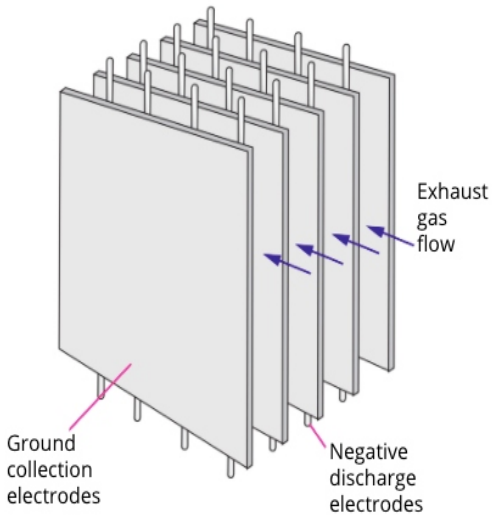

Figure 5. Electro filter components [37]

The primary gas treatment consists of either an electro filter or a bag filter. The exhaust gas from the boiler enters the bag filters, which capture particles from the exhaust gas. At regular intervals, the bag filters are blown in the opposite direction so that the particles such as fly ash which is a much finer type of ash, fall down to the bottom and are transported away for use in the production of cement, asphalt or are sent to landfills. Some incineration plants are equipped

with an electro filter to capture these fly ash particles. The exhaust gas particles receive a negative charge by means of negative discharge electrodes, and the particles are then drawn to ground collection electrodes. These are made up of thin plates that hang inside the electro filter, and work in the same way as a magnet. The plates are knocked in from time to time, which causes the dust to loosen and fall down as fly ash [38]. The treated exhaust gas then flows out of the filter system and goes to the secondary gas treatment.

2.2.4.2 Secondary gas treatment

The secondary gas treatment comes directly after the primary gas treatment and it consist of a wet scrubber and a catalytic converter.

i. Wet scrubber:

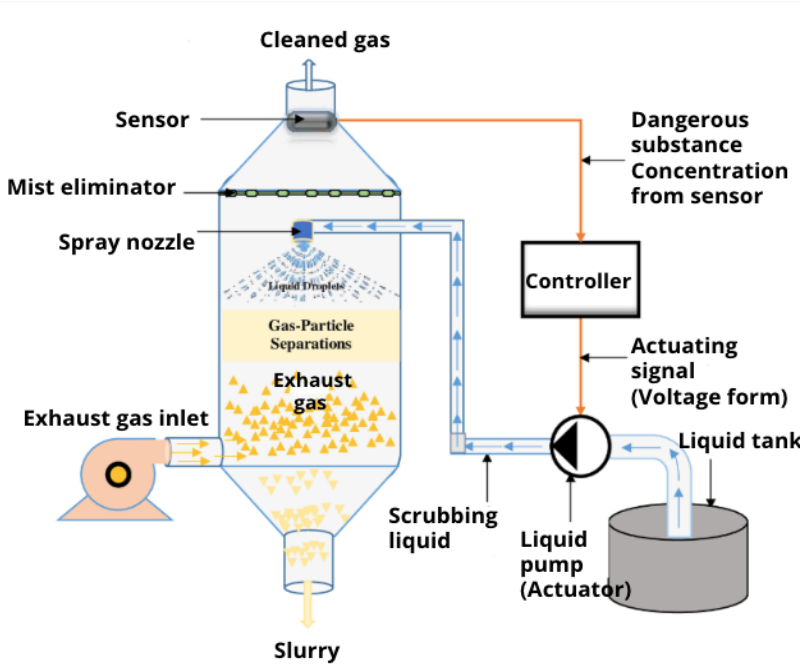

Figure 6. Schematic of Spray Tower Wet Scrubber System [39]

The exhaust gas undergoes a washing process in a large tower, where a scrubbing liquid comes from above and the exhaust gas goes into the tower from below. A pump transports the scrubbing liquid from a liquid tank into the scrubber and this liquid is then sprayed over the incoming exhaust gas through a spray nozzle. The scrubbing process occurs in the center of the scrubber where the scrubbing liquid collides with the exhaust gas. The scrubbing liquid will react with the pollutants in the exhaust gas and forms a slurry that falls to the bottom of the scrubber and goes out of the scrubbing tower. The cleaned gas then rises to the top of the scrubber; passing through a mist eliminator, which separates water droplets and moisture from

the gas before being sent to the next process. A sensor is installed on the top of the scrubbing tower to measure the concentrations of hazardous pollutants in the gas before the gas leaves the scrubber. The signal from the sensor is sent to the controller. Depending on pollutant levels and pollution standards, the controller can adjust the flow rate of the scrubbing liquid into the scrubber to achieve desired pollution levels.

The wet wash normally has four washing steps amongst which Activated Lignite Coke which is a form of activated charcoal is used. The activated charcoal can absorb dangerous substances in the exhaust gas such as dioxins, furans and mercury. In the final steps of the wet wash, hydrochloric acid (HCl), and sulfur dioxide (SO_2), are removed by pH adjustment. The slurry formed from the reaction of hazardous substances and scrubber liquid flows out of the scrubber from the bottom and is transported and purified in a separate treatment plant [38].

ii. Selective non-catalytic & selective catalytic reduction:

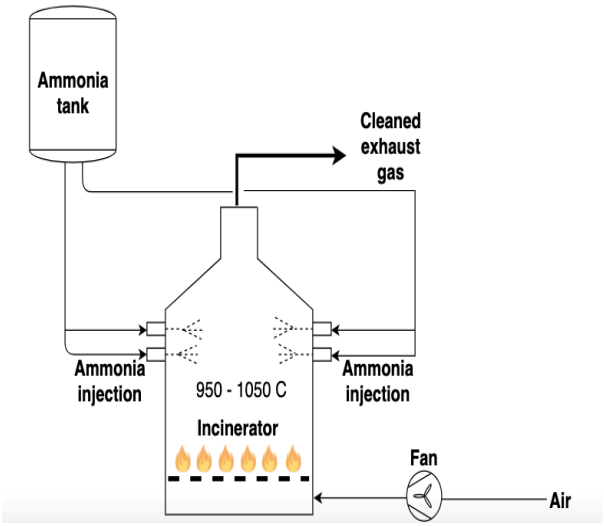

Figure 7. Selective non-catalytic reduction (SNCR)

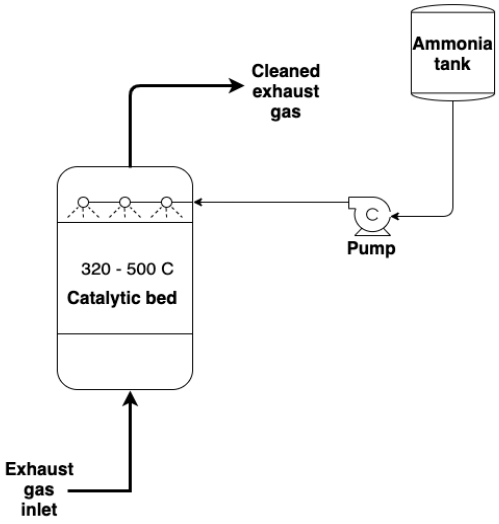

Figure 8. Selective catalytic reduction (SCR)

This is the final step for the cleaning of exhaust gases, to reduce the concentration of NO_X: nitric oxide (NO) and nitrogen dioxide (NO_2). This is done by adding ammonia (NH_3) using a catalyst. The catalyst allows the reaction before the NO_X reduction to take place at a lower temperature than would otherwise be necessary. This applies to newer plants which most often have the selective catalytic reduction (SCR) process. While the older plants mostly

have the selective non-catalytic reduction (SNCR) process where the NH_3 is added directly into the incinerator where the temperature is high [38]. This process can reduce NO_X gases into nitrogen (N_2) and water (H_2O) as presented by the two chemical equations below.

For NO_2, the following equation applies:

i. $2NO_2 + 4NH_3 + O_2 \rightarrow 3N_2 + 6H_2O$

For NO, the following equation applies:

ii. $4NO + 4NH_3 + O_2 \rightarrow 4N_2 + 6H_2O$

2.2.5 Exhaust gas release

Figure 9. Waste incineration plant with purified exhaust gas released into the atmosphere as water vapor [40].

The purified exhaust gas after leaving the secondary gas treatment process is released from about 80 meters high chimney into the air as water vapor. Measuring gauges are installed on the chimney to measure the quality of emitted gas continuously. The measuring results will provide a real-time control for the quality of emitted gas.

2.3 District heating distribution process

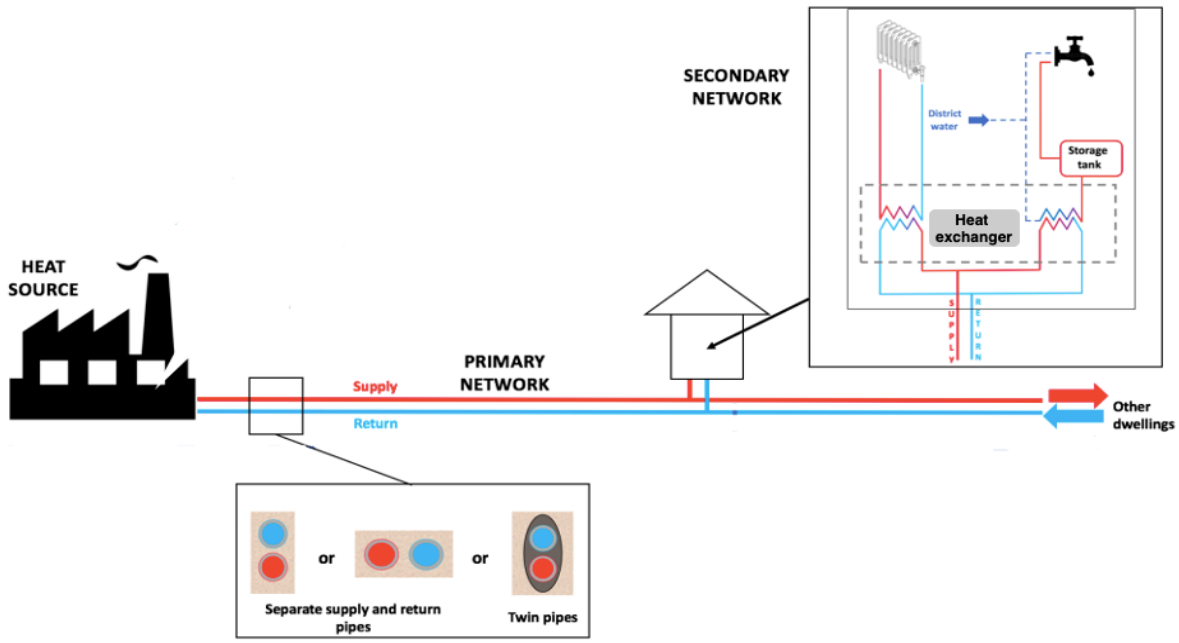

Figure 10. Schematic representation of a district heating network [41].

When the thermal energy is recovered from the exhaust gas and transferred over to the district heating water through a heat exchanger, the process continues its way through a network of insulated underground pipes which connect to client buildings to supply this energy. Figure 10 above shows the hot water supply in red leaving the plant on the primary network. Outlets from the primary network go to the secondary network which are found in client buildings. The secondary network recovers the energy from the primary network through a heat exchanger located in the client buildings as illustrated in Figure 10. The primary network cooled off water after the heat transfer makes its way back to the return pipe of the primary network, which leads to the plant in order to recover more energy. The secondary line after recovering energy from the primary line through the heat exchanger then makes its way to the heating radiators found in the various rooms of the building to supply heating. When the heating is supplied, the water returns to the heat exchanger cooled down in order to recover more energy and the process repeats itself. Apart from supplying heating to the various rooms in client buildings, some of the energy from the primary network is transferred through a heat exchanger into a second circuit in the secondary network which makes its way to a hot water storage tank and provides hot tap water to these buildings as shown in Figure 10. On the primary network the pipes are set up either with separate supply and return lines or twin pipes on a single line.

New client buildings interested in receiving district heating services get connected into the primary network for heating access.

2.4 District cooling

District cooling is the process by which cooling is produced and distributed from a centralized location. A district cooling system can reach an efficiency of 5-10 times higher than traditional local cooling systems [42]. The cold water for district cooling could be obtained from different free sources such as deep sea, lakes, rivers and aquifers. There are also industrial cooling sources where absorption chillers are used to achieve cooling such as trigeneration or combined cooling, heat and power (CCHP). This study will focus solely on cooling solutions, which require the use of low-grade waste heat in its production process.

2.4.1 District cooling production process

The district cooling production process starts with waste energy being recovered from a heat exchanger. In a waste incineration plant, this will occur at any stage between the exhaust gas leaving the incinerator and the exhaust gas entering the scrubber. The recovered energy can be used in a variety of options for cooling such as powering a steam-turbine drive centrifugal chiller or enabling refrigerant evaporation in a thermal compressor of an absorption chiller. Steam-turbine drive centrifugal chillers require high-grade waste heat in the form of steam and would be useful in plants with access to this. This however will not be considered in this study given it is not suited for the type of waste heat available to the plant in the case study. An absorption chiller instead will be considered in this study given that it requires low grade waste heat which is available to the plant in this case study.

2.4.1.1 Absorption chiller

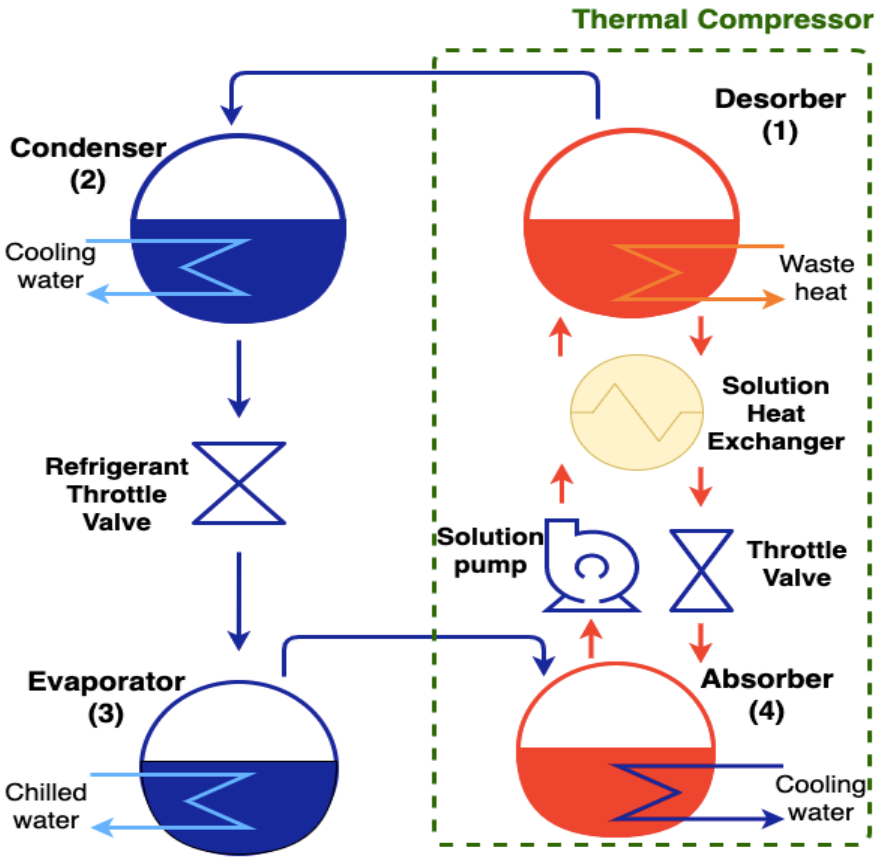

Figure 11. Single effect absorption chiller cycle with thermal compressor.

An absorption chiller is a type of chiller that provides cooling by using a thermal compressor which constitutes of an absorber, a solution pump, a throttle valve, a solution heat exchanger and a desorber. There are two cooling media pairs which are commonly used in absorption chillers: a mixture of NH_3 and H_2O, or LiBr and H_2O. Similar to a mechanical compressor in a vapor compression chiller, the thermal compressor takes low pressure, low temperature refrigerant vapor from the evaporator and delivers high pressure, high temperature refrigerant vapor to the condenser. The thermal compressor uses an absorbent fluid to chemically bond with the refrigerant vapor, compressing it by changing its phase from a gas to a liquid. The dilute solution of the refrigerant and absorbent is then pumped to the desorber passing through a solution heat exchanger for improved efficiency with the use of a reasonably small electric pump. When the dilute solution gets to the desorber, the refrigerant is boiled using thermal energy (waste heat) and it makes its way to the condenser. In the condenser, the refrigerant now in a vapor phase rejects heat to the cooling water and condenses back to a liquid phase in the process. The refrigerant liquid then is passed through a refrigerant throttle valve which reduces how much refrigerant passes through it at a time resulting to a drop in pressure and temperature

of the refrigerant before it heads to the evaporator. In the evaporator, the refrigerant is vaporized at low temperature by the water to be chilled, taking away heat from it, and resulting in a drop in temperature of the water. The chilled water is then transported through insulated pipes to provide cooling. The vaporized refrigerant makes its way to the absorber where it is absorbed into the refrigerant and absorbent solution, and pumped back to the desorber and the process repeats itself. The waste heat after transferring thermal energy to the desorber, returns to the plant exhausted, gets reheated and repeats the cycle. The cooling water on the other hand makes its way to a cooling source after collecting heat from the system, rejects the heat and returns to collect more heat from the system and the cycle restarts. Cooling sources may vary from plant to plant depending on location and preference and could be: air cooled cooling towers, water cooled cooling towers, ground source cooling, aquifer water cooling, sea water cooling, or river water cooling.

2.4.1.2 Plate heat exchanger

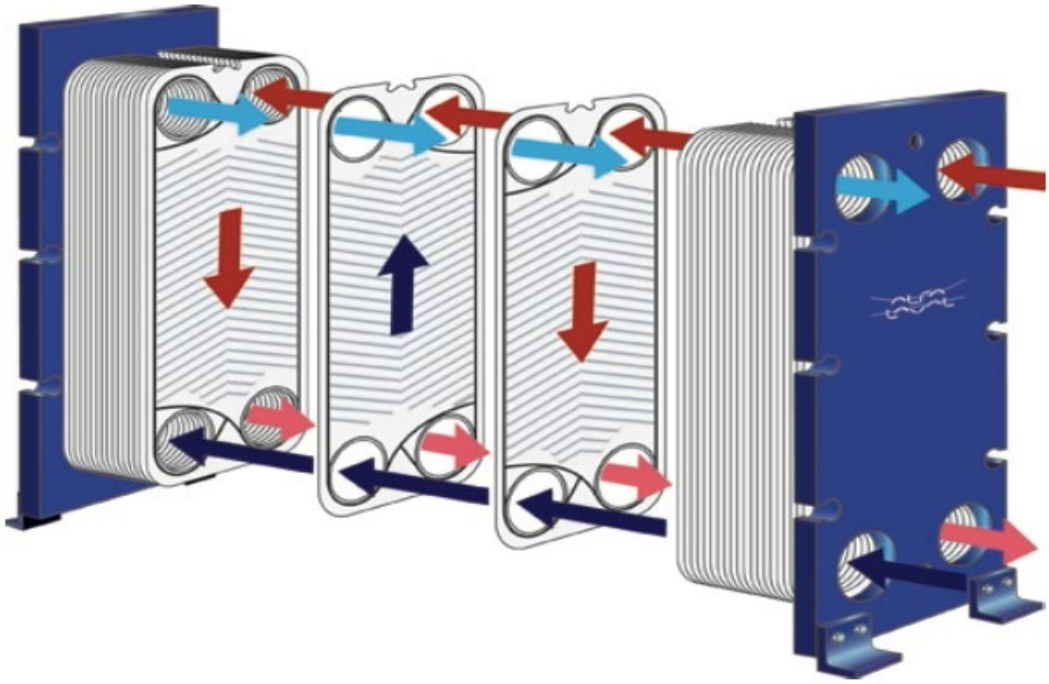

Figure 12. Plate heat exchanger components [43]

A plate heat exchanger is a common type of heat exchanger used in district heating and district cooling applications which require a liquid to liquid thermal energy transfer. A plate heat exchanger consists of a number of heat transfer plates which are held in place between a fixed plate and a loose pressure plate to form a complete unit. The heat exchanger has two separate channel systems whereby the fluids flow in counter-current flow and both fluids never come in

contact with each other. The plates are uneven on the surface, which creates turbulence in the fluids as they flow through the heat exchanger. The occurring turbulence, combined with the ratio of the volume of the media to the size of the heat exchanger, results in an effective heat transfer coefficient [43]. Figure 12 above shows the components of a plate heat exchanger with the fixed end plates at the edges, and the heat transfer plates in the middle. Single heat transfer plates are pulled together to form a plate pack, and the total heat transfer area of the heat exchanger is the sum of all the individual plate areas.

2.4.2 District cooling distribution process

The district cooling distribution process is similar to the district heating distribution process with a few minor differences.

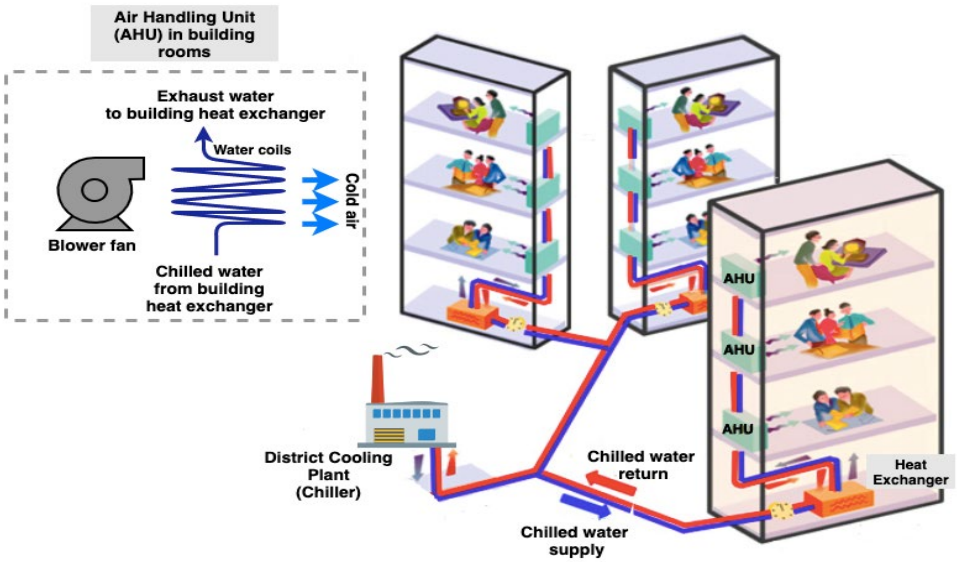

Figure 13. Schematic representation of a district cooling network [44].

The chilled water produced from the chiller leaves the plant on the primary supply line through insulated underground pipes. The primary line extends to customer buildings through a secondary line which connects to heat exchangers in these buildings. An internal closed water loop is cycled into the heat exchanger, where the water is chilled by water from the district cooling plant. The district cooling chill water returns to the plant on the return line after the thermal energy transfer for it to be re-chilled and the process restarts. The customer building´s internal water loop after being chilled, is supplied to the air handling units (AHU) located in the rooms that need cooling. As illustrated in Figure 13, the chilled water is run through the water coils of the AHU where a fan blows air over the coils resulting in the air being cooled

before entering the room. The exhaust water leaving the AHU water coil is sent back to the heat exchanger to be re-chilled and the cycle repeats itself.

3 Research methodology

This chapter provides a description of the research approaches, a description of the data collection and analysis process applied in order to achieve the research objectives of this study. In addition, this chapter presents the tools which were used to obtain the results of this work, and how the results were obtained.

The research approach in this study is a mixed research approach entailing a mixture of both the quantitative and the qualitative research approaches.

3.1 Data collection & analysis

In this study, quantitative data was mainly collected from Returkraft´s waste incineration plant. Quantitative data such as: monthly amount of waste burned, monthly thermal energy produced by the plant, monthly thermal energy consumption of the steam turbine, and monthly thermal energy consumption of the district heating network was collected for the years 2017, 2018 and 2019. Quantitative data of the Flakksvann water temperature was collected for every 30 minutes from June 2019 to June 2020 from the Norwegian Water Resource and Energy Directorate (NVE), as well as quantitative data in the form of prices for process equipment and piping installation was collected from several process equipment and service suppliers. The data was analyzed and possible areas for improvements within the system were put forward.

Computer programs were used in this study for simulations; to process the collected data mentioned above, and to plot this data into graphs. Firstly, the Python Pandas library version 1.0.3 [45] was used to process the data acquired from the NVE in order to obtain monthly average values.

The Python Matplotlib library version 3.2.1 [46] is a plotting library for the python [47] programming language and it was used to plot all the graphs in this study. The input data for plotting the graphs was the output from data manipulation with Pandas.

Furthermore, a script was written in MATLAB. version 9.6 (R2019a) [48] with relevant formulas, which was used to carry out heat transfer simulations across two water streams in four heat exchangers presented in chapter 5.1 of this study.

A model of a single effect LiBr-H_2O absorption chiller was built on ASPEN PLUS version 9.0 (2016) [49] to simulate how much cooling could be produced with the available waste heat that was recovered from the district heating system.

Finally, DRAW.IO [50] a free online diagram editor was used to build all the process flow and schematic diagrams which are presented in this study.

3.2 ASPEN PLUS model

A simulation model of an absorption chiller was built on ASPEN PLUS V9 based on C. Somers single effect LiBr absorption chiller model [51]. In ASPEN PLUS there are a wide range of property methods which are suited for various processes. The ELECNRTL (Electrolyte) property method was used in this simulation given it is better suited for reactions [51] which in this case is the association and dissociation of LiBr.

The model shown in Figure 15 consists of the main components of an absorption chiller being: an absorber, desorber, condenser, and evaporator (Figure 11). The visual differences come with the solution heat exchanger (SHX) which is modelled using two heater blocks which are connected to each other by a heat stream indicating that the heat rejected on the hot side will be added to the cold side. The condenser and evaporator are modelled similarly to the solution heat exchanger using two heater blocks to represent heat transfer from one to the other. The absorber was modelled using a heat exchanger with two inlet streams, one outlet stream, and heat transfer to a heater block. The desorber was modelled slightly differently. Given that ASPEN PLUS lacks a desorber in its component list, a series of components were put together to replicate the function of a desorber. Three heater blocks and a flash block were used to model the solution and refrigerant side of the desorber where the flash block is used to separate liquid solution from vapor refrigerant. Finally, given that ASPEN uses a sequential solver, it is essential to model a "break" in closed cycles so as to provide inputs to the model. Stream 1 and stream 1A are therefore not connected and if both streams provide the same results which is expected, given that they represent the same state, then this proves that the model converged and the problem was well formulated.

3.2.1 Assumptions made for the model

- Pump efficiency 100%
- Pump model assumes an adiabatic process (no heat is gained or lost by the system)

$$H_{in} = H_{out} \tag{3-1}$$

- No pressure drops on the heat exchanger
- No pressure drop on the condenser
- The refrigerant was assumed to leave the condenser as a saturated liquid
- No pressure drop in the evaporator
- Saturated vapor at the refrigerant exit of the evaporator.
- No pressure drop in the absorber
- Saturated liquid at the exit of the absorber
- Saturated liquid at the solution exit of the desorber (stream 4)
- Superheated vapor at the refrigerant exit of the desorber (stream 7)
- No pressure drop in the desorber
- Duty of the desorber is the sum of all individual desorber components.

$$Q_{Desorber} = \sum Q_{Desorber\ Components} \tag{3-2}$$

3.2.1.1 Input data

In order to run the simulation, desired inputs had to be inserted into the model. First was the mass fraction of LiBr and H_2O at stream 1 which were 0.57 and 0.43 respectively. The common weak solution values of LiBr-H_2O absorption chillers are in the range of (52-57%) [51-54]. A variety of concentration values were simulated, and the value of 0.57 representing 57% weak solution concentration of LiBr was chosen as it required a lower internal flow rate to achieve the desired chill water temperature of 7°C with an available waste heat hot water temperature of 85°C. This internal flow rate plays a role on the size of the chiller and the required work of the solution pump.

A LiBr-H_2O absorption refrigeration system works with very low operating pressures which are below atmospheric pressures. This is to permit the refrigerant (H_2O) to be able to evaporate and condense at lower temperatures than normal.

Given this, a low saturation temperature of the refrigerant was desired, which needs to be lower than the desired chill water outlet temperature to guarantee enough cooling to meet the desired chill water outlet temperature. From Figure 14, with a water saturation temperature of 5°C, the corresponding pressure is 0.87 kPa which was inserted as the low pressure input for the model. The optimum COP of a single effect absorption refrigeration cycle based on operating

temperature parameters has been studied by Salisu. L [55]. The condenser temperature range to maximize the COP of a single effect absorption chiller is between 32°C and 45°C. This corresponds to a H_2O saturation pressure in the range of about 4.5 kPa and 10 kPa from Figure 14 below. Given this, the high pressure or supply pressure of the solution pump was chosen to be 7.5 kPa which according Figure 14, would correspond to a water saturation temperature of about 42°C. Meaning the refrigerant will be at a superheated vapor phase at stream 7 after being heated up with a waste heat hot water temperature of 85°C and condense to its saturation temperature at stream 8 after the condenser.

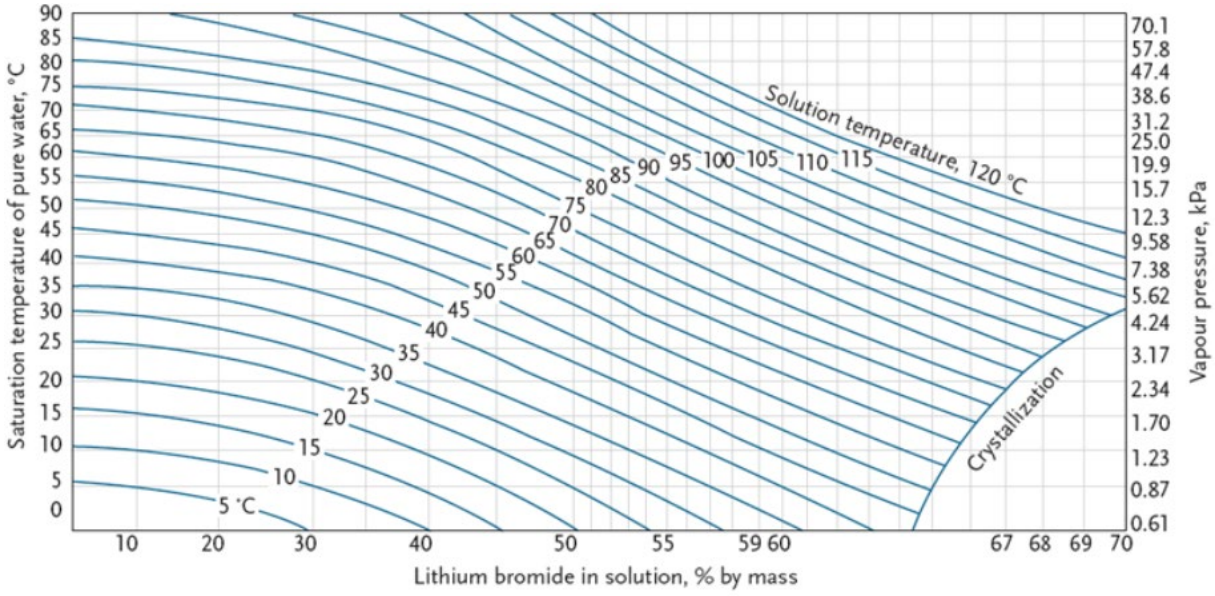

Figure 14. Temperature/ pressure/ concentration data for LiBr solution [56].

The lower the condensing water supply temperature, the more improved the efficiency of the chiller [57]. The idea when choosing the cooling water temperature for the condenser and absorber was to have a low enough temperature to benefit the efficiency of the chiller, but not low to the extent that would cause heat rejection issues to the available heat sink on the warmest days. Thus, the condenser and absorber cooling water temperatures were set to 25°C. The flow rate of the condenser cooling water, absorber cooling water, waste heat hot water, and chill water were suitable and reasonable values inputted to obtain desired results from the simulation.

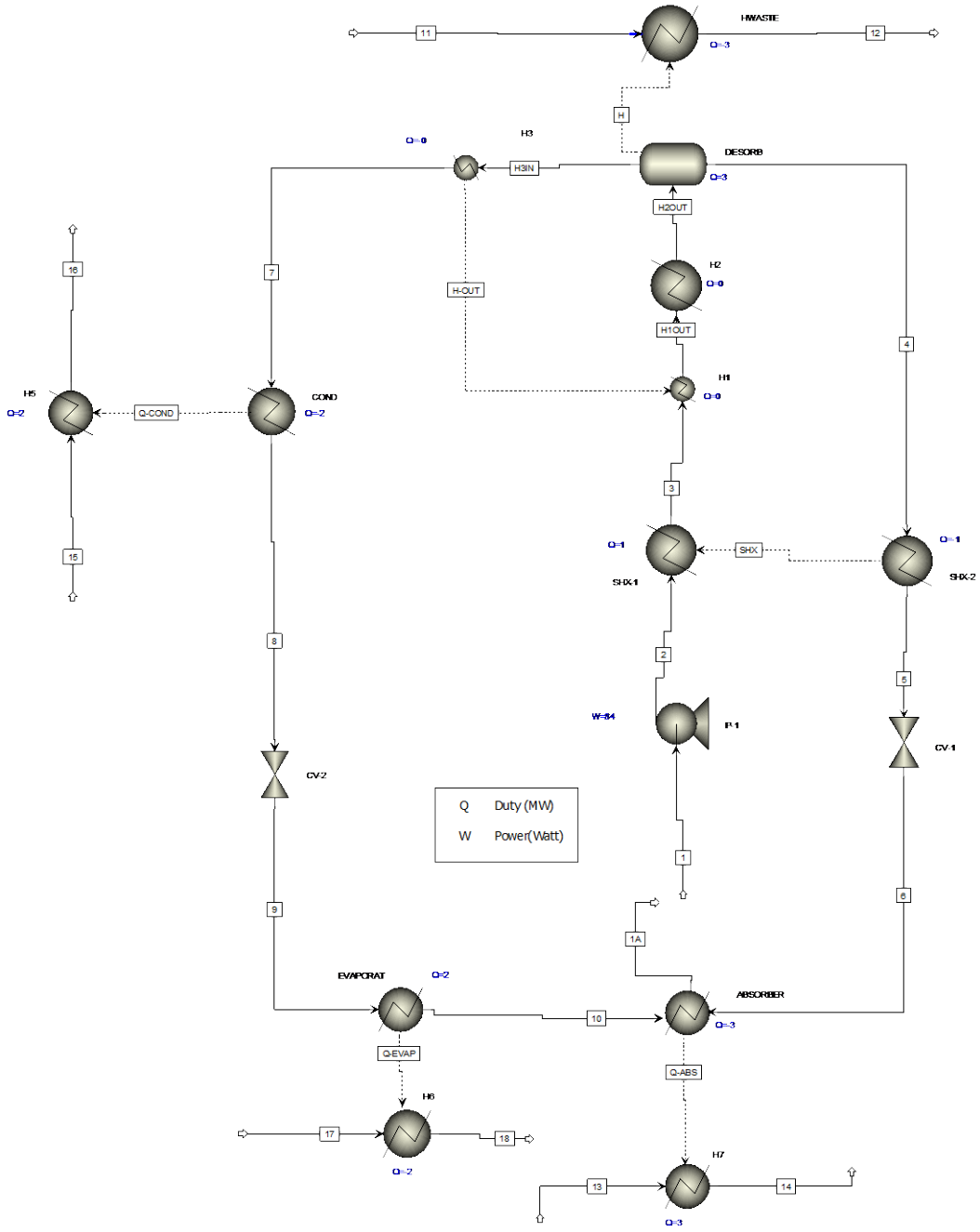

Figure 15. The model of a single effect LiBr-H_20 absorption chiller built on ASPEN PLUS.

3.3 MATLAB script

A script was written in MATLAB R2019a in order to calculate the unknown fluid properties in the counter-current flow plate heat exchangers which are presented later in this chapter. Appendix A shows the script which was written for the calculations. The script was based on the following equations and assumptions:

The thermal energy transfer equation as a result of the change in temperature. Where Q is the thermal energy in $\frac{KJ}{s}$, ṁ is the mass flow rate of the fluid in $\frac{Kg}{s}$, C_P is the specific heat capacity of the fluid in $\frac{KJ}{Kg*°C}$, and ΔT is the temperature change in °C.

$$Q = \dot{m} * C_P * \Delta T \tag{3-3}$$

The energy balance equation whereby heat removed from a hot stream is equal in magnitude to the heat absorbed by the cold stream.

$$-Q_{Hot} = Q_{Cold} \tag{3-4}$$

After calculating $-Q_{Hot}$ using equation (3-3), equation (3-4) is used together with equation (3-3) to find the unknown cold side temperature as presented in equation (3-5) below.

$$T_{Cold\ out} = \frac{Q_{Cold}}{\dot{m} * C_P} + T_{Cold\ in} \tag{3-5}$$

The heat transfer equation in a counter-current flow heat exchanger is given by equation (3-6). Whereby Q is the heat transfer across the two fluids in $\frac{J}{s}$ or W, U is the overall heat transfer coefficient in $\frac{W}{m^2*°C}$, and ΔT_{LMTD} is the logarithmic mean temperature difference in °C, and A is the heat transfer area of the heat exchanger in m^2.

$$Q = U * A * \Delta T_{LMTD} \tag{3-6}$$

The logarithmic mean temperature difference is given by equation (3-7).

$$\Delta T_{LMTD} = \frac{\Delta T_B - \Delta T_A}{Ln(\frac{\Delta T_B}{\Delta T_A})} \tag{3-7}$$

ΔT_A is the temperature change at one end of the heat exchanger and is given by equation (3-8).

$$\Delta T_A = T_{Hot\ out} - T_{cold\ in} \quad (3\text{-}8)$$

ΔT_B is the temperature change at the other end of the heat exchanger and is given by equation (3-9).

$$\Delta T_B = T_{Hot\ in} - T_{cold\ out} \quad (3\text{-}9)$$

U is the overall heat transfer coefficient of the heat exchanger and is given by equation (3-10) below. Whereby a_1 is the heat transfer coefficient between the warm medium and the heat transfer surface in $\frac{W}{m^2*°C}$, a_2 is the heat transfer coefficient between the heat transfer surface and the cold medium in $\frac{W}{m^2*°C}$, δ is the thickness of the heat transfer surface in m, R_f is the fouling factor in $\frac{m^2*°C}{W}$, and λ is the thermal conductivity of the material separating the medias in $\frac{W}{m*°C}$.

$$\frac{1}{U} = \frac{1}{a_1} + \frac{1}{a_2} + \frac{\delta}{\lambda} + R_f \quad (3\text{-}10)$$

The material type of the heat exchanger heat transfer plates and the thickness of the plates vary from manufacturer to manufacturer. The fouling factor and the fluid data (fluid turbulence) are unknown. It was therefore not possible to obtain the heat transfer coefficients, the thermal conductivity, and the thickness of the heat transfer surface in order to calculate the overall heat transfer coefficient U. As a result of this, the typical U-value or overall heat transfer coefficient (water/water) for a plate heat exchanger obtained from the plate heat exchanger manufacturer Alfa Laval is 6000 – 7500 $\frac{W}{m^2*°C}$ [43]. The average value of 6750$\frac{W}{m^2*°C}$ was used in the MATLAB script.

Finally using the energy balance equation (3-4) the calculated value of Q_{Cold} equals Q in equation (3-6). So the unknown variable which is the heat exchanger heat transfer area can be obtained by equation (3-11) below.

$$A = \frac{Q}{U * \Delta T_{LMTD}} \quad (3\text{-}11)$$

4 Case study

This chapter presents the case study of this thesis, a visual representation and discussion of the issue in question.

4.1 Returkraft AS

Returkraft AS is a waste incineration plant located in Langemyr, 5 km north of Kristiansand city center, in southern Norway. The plant was put into service in 2010 and incinerates about 130 000 tons of waste per year. Some of the energy recovered from the incineration process is used to produce 95 GW of electricity per year, which is equivalent to the electricity consumption for about 5000 homes. Also, some of the energy recovered from the incineration process is used to produce district heating which provides hot tap water and heating for about 12000 homes and companies.

Figure 16. Location of Returkraft´s plant in Kristiansand, southern Norway (Google maps, 2020) .

4.2 Plant setup

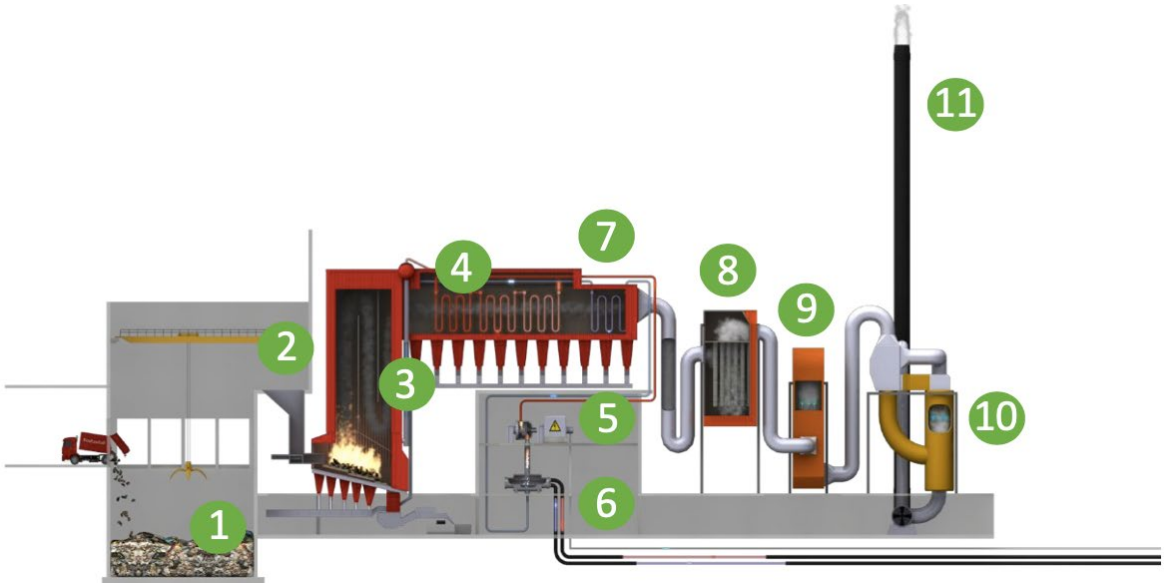

Figure 17. Illustration of Returkraft´s plant setup [58].

The process begins in stage (1) where between 30 to 50 waste container trucks deliver waste daily to the plant. At stage (2), the waste is fed to the filling funnel which leads the waste into the incinerator. The incinerator burns the waste in stage (3) at temperatures between 800 and 1000°C. Between 15 and 17 tons of waste are burned every hour. In the incinerator there are about 100 km of water pipes running along the walls. The pressure in these pipes is about 50 bar which enables water to start boiling at a temperature of 270°C. When the water turns into steam, it is forwarded into the boiler in stage (4) where the exhaust gas is at a temperature of about 550°C. This process converts the steam into dry superheated steam with a temperature of about 425°C which can be sent into the steam turbine. The dry superheated steam makes its way into the steam turbine in stage (5) where the turbine rotating at a speed of 8500 rpm, connected to a generator produces electricity which is sent to the electricity grid. The saturated exhaust steam which leaves the steam turbine is used to heat up district heating water in stage (6) through a heat exchanger. The district heating water enters the plant at a temperature between 50 – 60°C and leaves at a temperature between 80 – 130°C.

In stage (7), the exhaust gas from the incineration process depending on the type of waste, contains toxic components which need to be cleansed. This gas is transferred to the first of the three cleansing stages in stage (8). The plant has a bag filter installed in stage (8) where the exhaust gas is mixed with lime and activated carbon to capture toxic particles in the gas such as: dioxins and heavy metals. When the exhaust gas leaves this stage, it still contains NO_X gases which need to be cleansed. In stage (9) the plant has a SCR process where NO_X gases are

cleansed by adding NH_3 using a catalyst to achieve the reduction of NO_X gases into N_2 and H_2O. The exhaust gas then continues to the last cleansing stage (10) in a tower where is it washed with finely atomized water. This removes the rest of the heavy metals, HCL, SO_2 and regulates the exhaust gas temperature and pH levels. Finally, the exhaust gas which has been cleansed of all toxins is then released mainly as steam in stage (11) through a 75m tall chimney at a temperature of minimum 80°C.

4.3 Case description

Returkraft´s waste incineration plant generates a sizable amount of thermal energy from the waste incineration process. As illustrated in Figure 18 below, the plant averagely produces about 29 274 MWh of thermal energy each month, throughout the entire year from waste through its incinerator and boiler in the course of the incineration process. Figure 18 further shows that the electricity production through the steam turbine is relatively constant throughout the year with the turbine consuming an average value of about 7 424 MWh of thermal energy each month. It is noticeable that during the coldest months of the year from November to March, about 15 094 MWh of thermal energy is averagely consumed by the district heating network each month to provide hot tap water and heating to homes and companies. After the coldest months, the demand for heating decreases on the client´s side and so does the amount of thermal energy consumed in the district heating network by the client buildings. During the warmest months of the year from May to September, the average amount of thermal energy consumed by the district heating network is only about 4258 MWh every month.

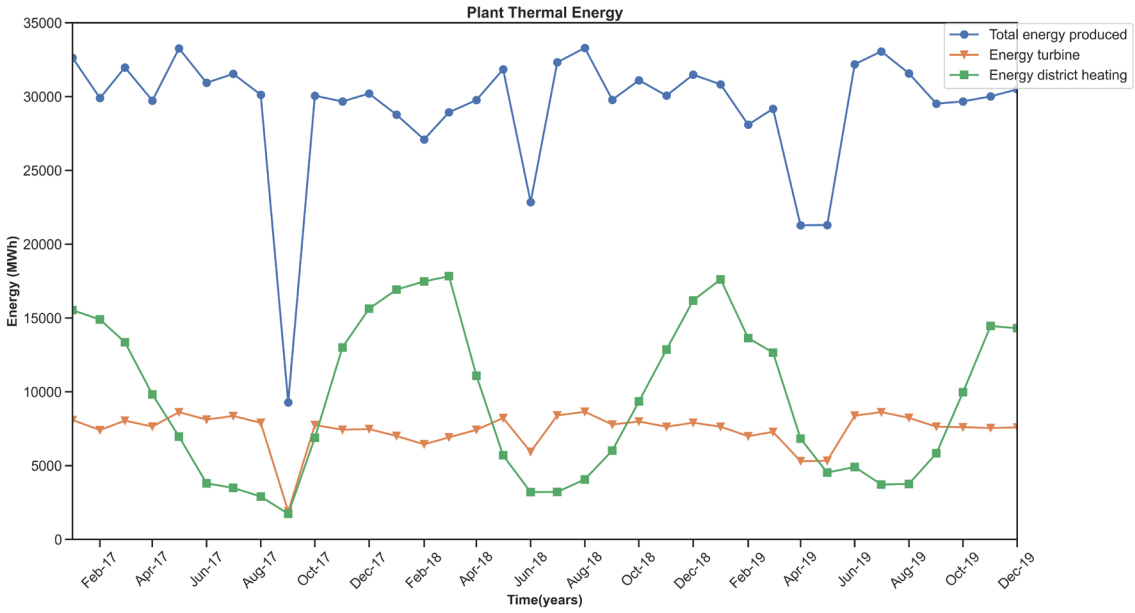

Figure 18. Thermal energy production and consumption of Returkraft´s plant from January 2017 to December 2019.

The amount of waste burned by the plant every month is averagely about 11 396 tons of waste and has little variations throughout the year. Figure 19 below illustrates the amount of waste which was burned monthly in the plant from January 2017 to December 2019. There are some deviations in September 2017, June 2018, April and May of 2019 but otherwise the values are fairly constant.

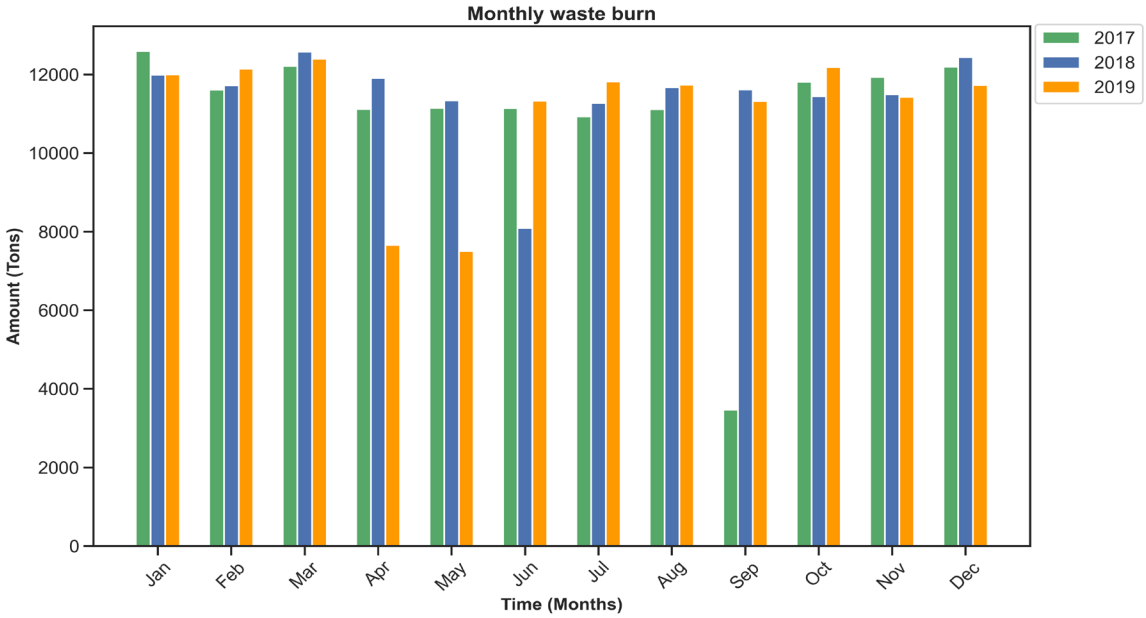

Figure 19. Monthly amount of waste burned by Returkraft´s plant from January 2017 to December 2019.

With a constant amount of waste being burned in the plant every month, the amount of thermal energy produced from the waste, and the amount of thermal energy consumed by the steam turbine for electricity production are also constant. The only discrepancy is the district heating network consumption. Figure 20 below illustrates the amount of recovered thermal energy from the waste incineration process that is being used during the various months of the years 2017, 2018 and 2019. It is noticeable from Figure 20 that during the coldest months of the year (November – March), there is averagely about 76% utilization of the thermal energy produced from the waste incineration process. During the warmer months of the year (May – September), there is averagely only about 41% of the thermal energy produced from the waste incineration process which is being used.

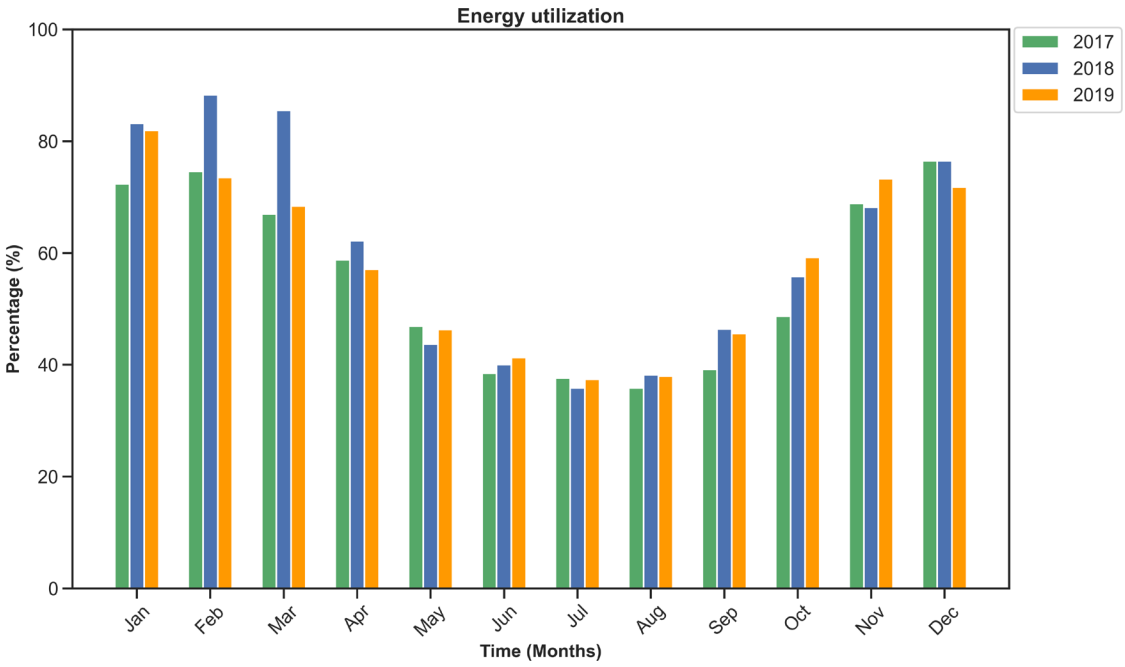

Figure 20. Monthly energy utilization of Returkraft´s plant for the years 2017, 2018 and 2019.

These low percentages of energy utilization in the warmer months of the year correspond with the increasingly warmer climatic conditions during these months and the associated decrease in the demand for heating. This is also owed to the increasingly tighter regulations surrounding the construction of more efficient buildings [59] with better insulation capabilities, thereby reducing the need for excessive heating. As a result, a lot of the thermal energy that cannot be consumed in the district heating network is wasted by being cooled off to ambient air. Figure 21 and Figure 22 show the condenser fans which are 28 in total, being used to discard the

thermal energy that cannot be consumed in the district heating network on the warmer months of the year.

Figure 21.Condenser fans on the roof at Returkraft´s plant used to discard excess thermal energy on the warmer months of the year. Photo: Tormod Flem Vegge [60].

Figure 22. Aerial view of the condenser fans on the roof at Returkraft´s plant [61].

With the use of the condenser fans, the threshold of about 10 836 MWh of thermal energy averagely each month is being discarded to ambient air between May and September every year. Figure 23 below shows an overlaid graph of the monthly thermal energy consumed by the district heating network for the years 2017, 2018 and 2019. The overlaid graphs emphasize on the severity of the recurrent threshold illustrated in the figure, representing the amount of thermal energy being discarded to ambient air during the warmer months of the year which could otherwise be put to better use in another process.

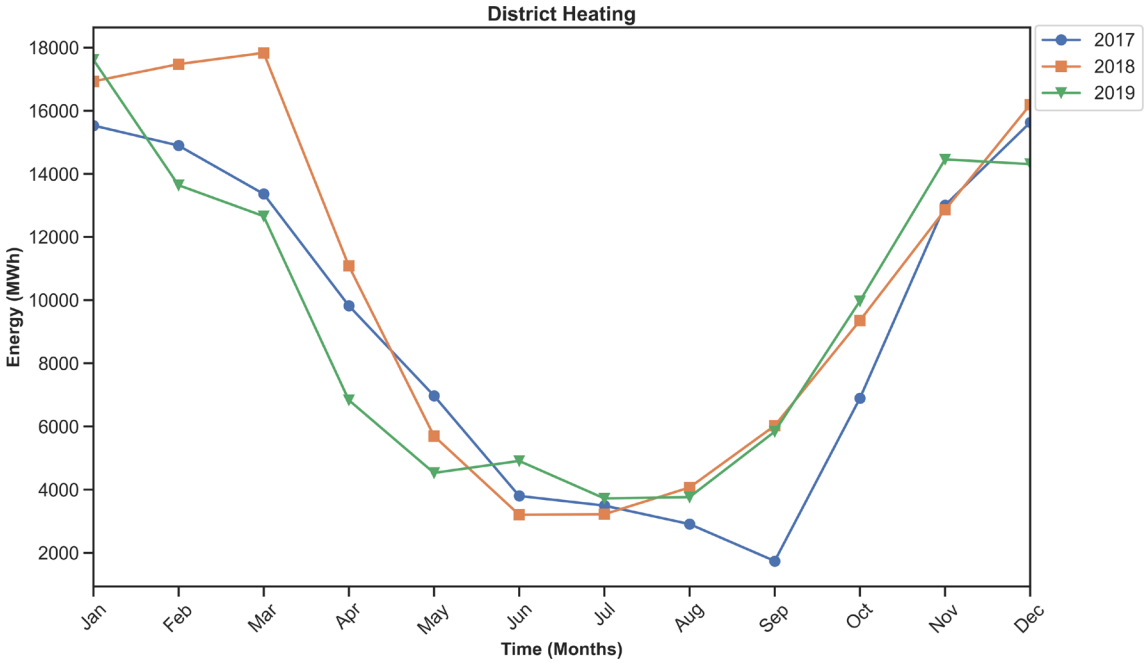

Figure 23. District heating thermal energy overlaid for the years 2017, 2018 and 2019.

The energy not consumed by the district heating network is rejected to ambient air in order to maximize heat transfer. Figure 24 below presents the high pressure condenser (HP-Cond) and the low pressure condenser (LP-Cond) where the transfer of thermal energy from the steam condensate to the district heating return water occurs. In order to maximize the heat transfer in the LP and HP- Cond, the temperature difference between the return district heating water and the temperature in the LP and HP- Cond need to be as large as possible. Given this, on very warm summer days with an ambient temperature of about 25°C when there is little demand for heating, the return temperature of the district heating water can be 60°C. With a temperature difference of just 35°C, a larger heat transfer area of the heat exchanger and additional condenser fans will be required in order to remove the heat from the system and lower the return water temperature to 50°C. Due to this, Returkraft sends a separate stream from the hot district heating supply line which can sometimes be 100°C through the heat exchanger to be cooled down to a glycol cycle and ambient air. At this point, better heat exchanger efficiency will be achieved given a temperature difference of 75°C at ambient temperatures of 25°C. The cooled down district heating supply water now at a lower temperature than the district heating return water can be mixed into the district heating return water stream to achieve the desired temperature as illustrated in Figure 24 below. Although this achieves better heat transfer at the

level of the LP-Cond, HP-Cond, and the glycol heat exchanger cycle, a lot of thermal energy gets discarded in the process thereby reducing the overall efficiency of the plant.

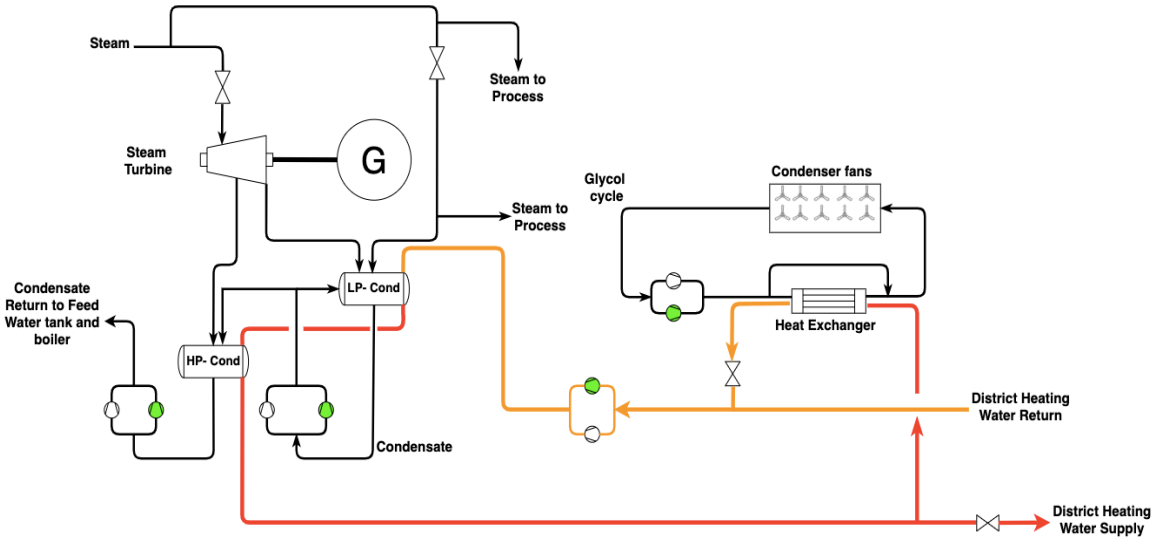

Figure 24. Simplified schematic of Returkraft´s thermal energy transfer to and from district heating water.

5 Results and discussion

This chapter presents the obtained research results and the discussion of these obtained results.

5.1 Proposed system approach

With increasing ambient temperatures in the summer, the cooling demand increases as well. The system proposed is to put the waste thermal energy to a use such as cooling which will be beneficial to the residents of the city of Kristiansand during the period of low heating demand in the summer and early autumn.

The proposed system is approached by analyzing Returkraft´s production data for the past three years, to visualize a pattern and establish how much thermal energy is being wasted and how it could be put to better use during the summer and autumn seasons. Moreover, suggesting cooling solutions which require the use of low grade thermal energy for its operation such as an absorption chiller, is ideal for a waste incineration plant with an excess of low grade waste heat. Achieving cooling requires some analysis being done on the heat recovery system of the plant to propose a system which can easily be incorporated into the existing plant, without obstructing normal production.

5.2 Proposed system

To address the efficiency of Returkraft´s plant during the warmer months of the year, some changes to the setup of the plant have been considered. The proposed system was aimed at providing utilization to the otherwise wasted thermal energy while minimizing the amount of changes required to be made to the existing setup in order to achieve this goal. Compared to the plant setup illustrated in Figure 24, the proposed system presented in Figure 25 below completely excludes the glycol cycle and the condenser fans which reject heat to ambient air.

The system maintains the district heating supply hot water stream which used to be routed through the glycol heat exchanger in order to cool down the district heating water return stream. That stream is indicated by a (red) line and it is sent through a heat exchanger (HX3), and on the counter flow side of HX3 is a cool water stream (dark blue) line at the temperature of 25°C which will need to be heated and used to drive the absorption chiller. The cool water stream gets heated up, resulting to a drop in temperature of the hot water stream now an orange line after HX3. The now cooled-off district heating water supply stream is forwarded to the district heating water return stream and its flow rate is regulated by a control valve to cool down the district heating water return stream to the desired temperature.

Given the district heating network set-point temperature is decided upon based on ambient temperatures and consumption in the network, the district heating hot water supply temperature can vary in the range of (80-130°C) as mentioned in chapter 4.2. As a result , the district heating hot water supply stream being sent to HX3 will also vary. At the time of writing this thesis (July 2020), the set-point temperature is at 90°C. Given this, the setpoint temperatures of 80°C and 90°C were simulated and will be presented later in this chapter. If the set-point temperature hot water stream sent to HX3 is high enough to raise the cool water temperature from 25°C to the desired driving temperature of the chiller desorber after leaving HX3, the cool water stream now hot will bypass HX4 using the bypass stream and head to the chiller. In the scenario whereby the set-point temperature hot water stream sent to HX3 is not high enough, the cool water stream now warm will be forwarded through HX4 whereby it will be additionally heated by hot condensate the (black) line leaving HP-Cond and routed through HX4. The hot condensate will be routed through its HX4 bypass stream when additional heating is not required.

The hot water (dark blue) line after transferring its thermal energy to the chiller to produce cooling will need to be cooled down back to 25°C for the process to restart. The same applies to the hot water stream from the chiller condenser and absorber the (orange) lines. Given the minimal difference in hot water exit temperatures of the chiller condenser and absorber, both streams can be merged into one stream, cooled down and split up again into two streams.

The presented solution for cooling these streams is river water instead of a traditional evaporative cooling tower. This selection was made because of the high operational costs from excessive municipality fresh water consumption or high raw water treatment costs on the plant due to evaporation in the cooling tower for heat dissipation.

River water will therefore be pumped as a single main-stream from the river bottom. A smaller stream will be routed off the main-stream into HX1 to cool down the chiller condenser and absorber hot water while the remaining stream will be forwarded to HX2 to cool down the chiller desorber hot water. When the river water after leaving HX1 and HX2 will be merged back into one main-stream and pumped back into the river for the process to restart. The cooled off desorber water leaves HX2 and is forwarded back to HX3 for the process to restart. At the same time the cooled off chiller condenser and absorber water return to the chiller and the process restarts.

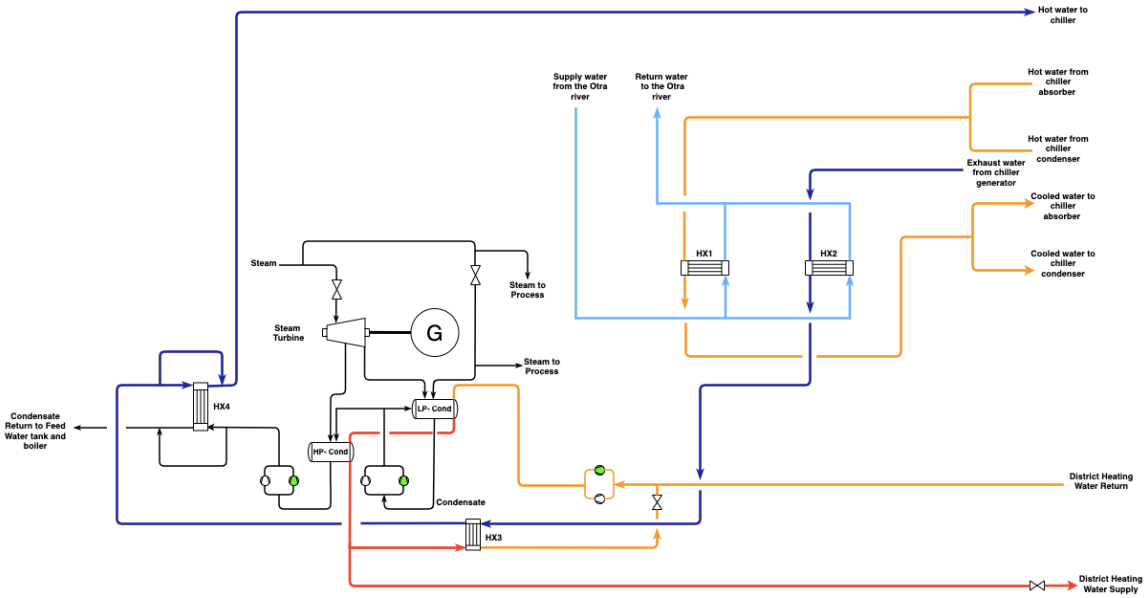

Figure 25. Proposed alternative setup of Returkraft´s plant in Langemyr.

5.2.1 Otra River

The Otra river is the 7th longest river in Norway with a length of 240 km. The river is located in the Agder county and stretches from Setesdalen to Kristiansand. It has been used for hydro-power production since the 1890s and per 2015, there are all together 22 small and large scale hydro-power stations with a yearly electricity production of 4258 GWh [62, 63].

The Otra river was chosen as a heat sink for the proposed system because it is the closest water body to the plant which could be used for this purpose. Figure 26 below illustrates the location of Returkraft´s plant with the red mark and the direct distance to the Otra river presented by the white line which is 1.30 km.

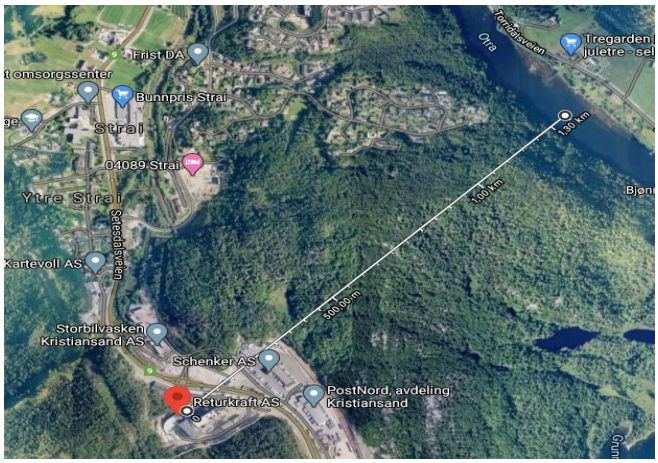

Figure 26. Direct distance from Returkraft´s plant in Langemyr to the Otra river (Google satellite, 2020).

Given the lack of measured temperature data available for this river, it was necessary to establish a reasonable assumption for the monthly average temperatures in order to progress with this study.

5.2.2 Flakksvann

Flakksvann is part of the Tovdalselva river and is a situated in the Birkenes municipality which is also part of the Agder county. The water body according to Google maps 2020 is at a direct distance of about 22 km to the Otra river and about 23 km to Returkraft´s plant. This was the closest water body to the Otra river with measured water temperature data. This data was provided by the NVE who records the temperature readings every half-hour for an entire year. The monthly average of this data for the period May 2019 to May 2020 is plotted in Figure 27 below. The highest value (19°C) corresponding to the highest average temperature of the water was used in the calculations of this study, given it will represent the average water temperature on the warmest month of the year. This data was used to represent the Otra river water temperature based on the assumption that both water bodies are in very close geographical proximity to each other and are subjected to the same climatic conditions which affect the water temperatures.

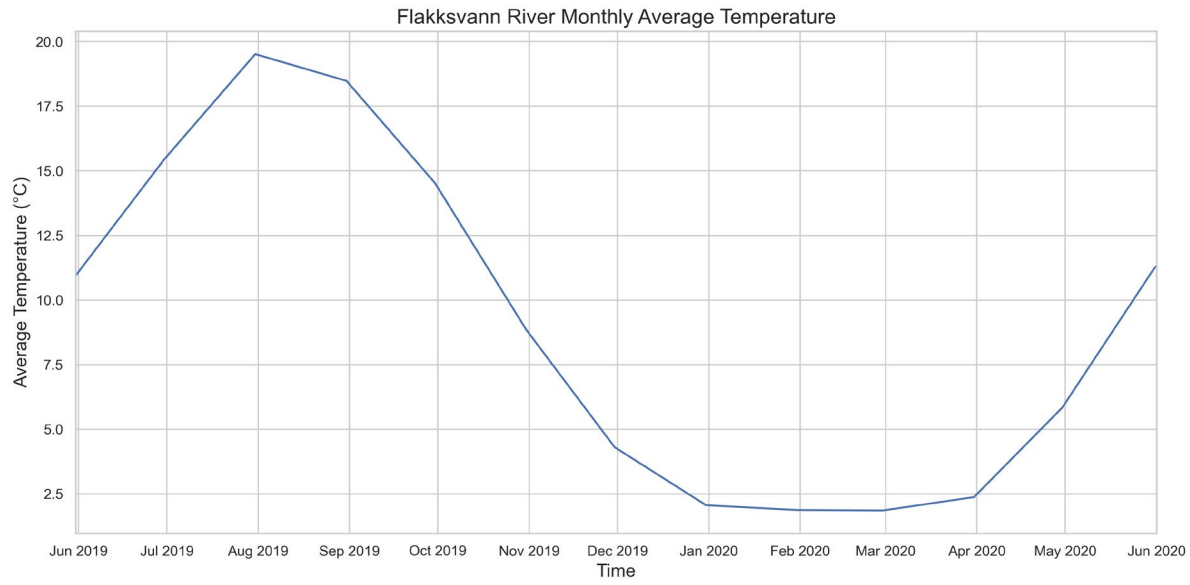

Figure 27. Average monthly water temperatures of the Flakksvann (NVE data).

5.2.3 District heating network set point temperature 90°C

In order to easily integrate the proposed system into the existing plant, it was necessary to simulate using normal production data in order to achieve the desired results. The warmer months as stated in chapter 4.3 go from May to September. Given the set point temperature at the time of writing this thesis (July 2020) is 90°C, it assumed that the set-point temperature during the warmer months will mainly range between 80°C and 90°C. As a result of this, the simulations were made based on the district heating supply water set-point of 80°C and 90°C.

Furthermore, the temperature chosen for the hot water being supplied to the chiller desorber was 85°C. This temperature was chosen because it facilitates the incorporation of the proposed system with existing set-point water and condensate temperatures in the plant.

5.2.3.1 Set-point 90°C, HX3

Table 2 below shows the input data and the results from the MATLAB script for the heat exchanger (HX3). The yellow color code represents the default flow rate values of the plant and the corresponding results. The green color code represents the proposed values for the system with the corresponding results. The desorber drive water stream was given a flow rate of 78 kg/s in the ASPEN PLUS chiller simulation. The same flow rate is used for this stream through HX3 with an inlet temperature of 25°C. The district heating hot water supply stream

previously being sent to the glycol cycle had a flow rate of 112 kg/s, this value is put into the MATLAB script together with an inlet temperature of 90°C and a desired outlet temperature of 45°C as presented with the yellow color code. These inputs presented a cold stream outlet temperature of 89.6 °C meaning the cold stream will be heated up to the initial temperature of the hot stream. Ideally that is possible but not very realistic. So the flow rate of the hot stream was reduced to 95 kg/s and the desired hot stream outlet temperature was lowered to 40°C. The reduction in flow rate and desired hot stream outlet temperature adjusted the amount of heat transfer required to provide the desired outlet temperature of the cold stream of 85.8°C as presented in the green color code. Because the exit temperature of the cold stream exiting HX3 already attained the desired chiller desorber temperature of 85°C, there is no need for additional heating so the stream is forwarded directly to the chiller. Finally, given the proposed hot stream and cold stream fluid properties across HX3 resulted in a calculated thermal energy transfer of $1.9865*10^4$ KJ/s, the required heat transfer area for HX3 will need to be 284 m^2.

Table 2. Input data and results of the MATLAB simulation for HX3 at a set-point temperature of 90°C.

HX3 (Set point 90°C)	Hot Stream in	Hot Stream out	Cold stream in	Cold stream out
Mass flow rate (Kg/s)	112	112	78	78
Temperature (°C)	90	45	25	89.6
Thermal Energy Transfer (KJ/s)	$2.1077*10^4$			
Required Heat Exchanger Area (m^2)	629			
Mass flow rate (Kg/s)	95	95	78	78
Temperature (°C)	90	40	25	85.8
Thermal Energy Transfer (KJ/s)	$1.9865*10^4$			
Required Heat Exchanger Area (m^2)	284			

5.2.3.2 Set-point 90°C, HX2

When the 85.8°C water is sent to the chiller, it leaves at a temperature of 75.1°C which is the hot stream inlet temperature at HX2 as presented in Table 3. The hot stream desired outlet temperature of 25°C is used, the flow rate is maintained at 78 kg/s and the Otra river hottest month average temperature of 19°C is used as the cold stream inlet temperature. With a cold stream flow rate of 100 kg/s, the desired hot stream outlet temperature was achieved and the calculated thermal energy transfer was $1.6342*10^4$KJ/s with a required heat exchanger area of 230 m^2 for HX2. The cold stream has an outlet temperature of 58°C and is pumped back into the river.

Table 3. Input data and results of the MATLAB simulation for HX2 at a set-point temperature of 90°C

HX2 (Set point 90°C)	Hot Stream in	Hot Stream out	Cold stream in	Cold stream out
Mass flow rate (Kg/s)	78	78	100	100
Temperature (°C)	75.1	25	19	58
Thermal Energy Transfer (KJ/s)	$1.6342*10^4$			
Required Heat Exchanger Area (m^2)	230			

5.2.3.3 Set-point 90°C, HX1

An inlet water temperature of 25°C was used for the chiller condenser and absorber in the ASPEN PLUS simulation. This provided a condenser outlet temperature of about 32°C and an absorber outlet temperature of about 34°C. Given both streams are water, have the same inlet temperatures and have minimal outlet temperature differences, both streams could be merged into one stream in order to enable the use of a single heat exchanger instead of two for this purpose. In order to achieve this, the diameter of the merged single pipe will have to be increased accordingly and should provide approximately the same flow rate. After the cooling, both streams will be split up again into two streams and forwarded back to the chiller condenser and absorber. The hot stream inlet temperature for HX1 was chosen to be an average of the outlet water temperatures of the chiller condenser and absorber. This was logical given they are the same type of fluid, have the same flow rate and when mixed, should have a final temperature between 32°C and 34°C. Given this, the hot stream inlet temperature of 33°C together with a flow rate of 80 kg/s was used in the MATLAB calculation. The river cooling water temperature of 19°C was used for the cold stream inlet temperature with a flow rate of 60 kg/s which was able to cool down the hot stream to the desired outlet temperature of 25°C. The cold stream (river water) outlet temperature was 29.6°C and finally the calculated thermal energy transfer was $2.6765*10^3$ KJ/s which requires a heat transfer area of 88 m^2 for HX1 as presented in Table 4 below.

Table 4. Input data and results of the MATLAB simulation for HX1 at a set-point temperature of 90°C

HX1 (Set point 90°C)	Hot Stream in	Hot Stream out	Cold stream in	Cold stream out
Mass flow rate (Kg/s)	80	80	60	60
Temperature (°C)	33	25	19	29.6
Thermal Energy Transfer (KJ/s)	$2.6765*10^3$			
Required Heat Exchanger Area (m^2)	88			

5.2.4 District heating network set point temperature 80°C

The district heating network set point of 80°C is the minimum set point temperature, which logically is implemented during the period with warm ambient temperatures and the least consumption on the network which falls within the scope of this study. Given this, it was necessary to simulate the possibility of cooling production with this set point temperature.

5.2.4.1 Set-point 80°C, HX1

No changes were made to the hot stream flow rate, and outlet temperature compared to the proposed values presented in Table 2. The same applies to the cold stream inlet temperature and flow rate. The aim here was to minimize changes to operational values where possible and maintain a stable operation despite the changes in set point temperatures. The only change made was to the hot stream inlet temperature which is the set point temperature of 80°C which provided a cold stream outlet temperature of 73.7°C as shown in Table 5. The thermal energy transfer calculated was $1.5892*10^4$ KJ/s which requires a heat transfer area of 236 m^2 for HX1.

Table 5. Input data and results of the MATLAB simulation for HX1 at a set-point temperature of 80°C

HX3 (Set point 80°C)	Hot Stream in	Hot Stream out	Cold stream in	Cold stream out
Mass flow rate (Kg/s)	95	95	78	78
Temperature (°C)	80	40	25	73.7
Thermal Energy Transfer (KJ/s)	$1.5892*10^4$			
Required Heat Exchanger Area (m^2)	236			

5.2.4.2 Set-point 80°C, HX4

Given the set point temperature of 80°C and the desired chiller desorber hot water temperature of 85°C, it was necessary to find an additional source of heating which would demand the use of an extra heat exchanger. The cold fluid leaving HX3 has an outlet temperature of 73.7°C and a flow rate of 78 kg/s. These values are used as the cold fluid inlet properties to HX4. The additional heat source comes from the condensate outlet stream leaving HP-Cond has shown in Figure 24 and Figure 25 above. This stream normally has a flow rate of 17 kg/s and temperature of about 90°C. The 90°C condensate stream is pumped to the feed water tank and later to the boiler for steam production with and inlet temperature of about 90°C. When choosing the outlet temperature of the hot stream for HX4, the idea was to lower the temperature to a value not considerably far from the boiler inlet temperature of 90°C. So the HX4 hot stream outlet temperature of 76°C was used for the calculation as presented by the yellow cell in Table 6 below. This resulted in a cold stream outlet temperature of only 76.75°C, a thermal energy transfer of 995.31 KJ/ and required heat transfer area of 24 m^2 for HX4. Given the cold stream outlet temperature was about 8°C short of the desired temperature of 85°C, it was necessary to increase the flow rate of the hot stream to achieve the desired cold stream outlet temperature. The hot stream flow rate was therefore increased to 65 kg/s which provided a cold stream outlet temperature of 85.3°C, a thermal heat transfer of $3.8056*10^3$ KJ/s and a required heat transfer area of 170 m^2 for HX4 as presented in the green cells in Table 6.

Table 6. Input data and results of the MATLAB simulation for HX4 at a set-point temperature of 80°C

HX4 (Set point 80°C)	Hot Stream in	Hot Stream out	Cold stream in	Cold stream out
Mass flow rate (Kg/s)	17	17	78	78
Temperature (°C)	90	76	73.7	76.75
Thermal Energy Transfer (KJ/s)	995.3160			
Required Heat Exchanger Area (m^2)	24			
Mass flow rate (Kg/s)	65	65	78	78
Temperature (°C)	90	76	73.7	85.3
Thermal Energy Transfer (KJ/s)	$3.8056*10^3$			
Required Heat Exchanger Area (m^2)	170			

5.2.4.3 Set-point 80°C, HX1 & HX2

Since the chiller desorber hot water inlet temperature is already at the desired drive temperature of 85°C, the rest of the process for HX1 and HX2 for the 80°C set point temperature is exactly the same as that of the 90°C set point temperature which was presented in Table 3 and Table 4 above.

5.2.5 LiBr-H_20 absorption chiller refrigeration cycle

Table 7 below presents the input data and the results generated by the ASPEN PLUS model which will provide further comprehension of the simulation. The table shows how the internal flow rate, temperature, pressure, phase, and concentration of the refrigerant and absorbent vary with every step of the refrigeration cycle. Besides the input values mentioned in chapter 3.2.1.1, all other values presented in Table 7 were generated by ASPEN PLUS.

Table 7.Input data and results of the LiBr-H_20 absorption chiller simulation on ASPEN PLUS.

	Units of Measurement	1	2	3	4
From		Absorber	Pump	SHX	Desorber
To		Pump	SHX	Desorber	SHX
Pressure	kPa	0.87	7.5	7.5	7.5
Temperature	°C	36.3	36.3	67.7	84
Mass Flow rate	kg/s	20	20	20	19.001
Vapor Quality		0	0	1	0
LiBr Concentration		57%	57%	57%	60%

	Units of Measurement	5	6	7	8
From		SHX	Valve	Desorber	Condenser
To		Valve	Absorber	Condenser	Valve
Pressure	kPa	7.5	0.87	7.5	7.5
Temperature	°C	50	42.28	74	40.22
Mass Flow rate	kg/s	19.001	19.001	0.99	0.99
Vapor Quality		0	0.0055	1	0

LiBr Concentration		60%	60%	0%	0%

	Units of Measurement	9	10
From		Valve	Evaporator
To		Evaporator	Absorber
Pressure	kPa	0.87	0.87
Temperature	°C	4.87	4.87
Mass Flow rate	kg/s	0.99	0.99
Vapor Quality		0.059	1
LiBr Concentration		0%	0%

5.2.6 LiBr-H_20 absorption chiller component data and results

The aim of the simulation was finding out how much cooling could be achieved given the amount of waste thermal energy being supplied to the chiller desorber. This involved making the most out the waste heat hot water stream. An increase in the internal flow rate of the refrigeration cycle provided a drop in the outlet temperature of the waste heat hot water leaving the chiller desorber, and consequently an increase in the desorber and evaporator duty. This also affected the chill water temperature leaving the evaporator which dropped lower than the normal district cooling chill water temperature range of 4°C and 9°C [64, 65]. Moreover, higher costs are incurred on piping and pump work with higher flow rates [66] thereby impacting the total cost of the chiller. Given this, reducing the weak solution concentration provided a better duty on the evaporator and desorber enabling the internal flow rate to be slightly reduced together with the pump work while achieving desired chill water temperatures and acceptable duties. Nevertheless it was necessary to look out for the strong LiBr solution concentration

generated by ASPEN PLUS since a concentration of 65% and above combined with the selected low pressure of 0.87 kPa will result in the crystallization of LiBr as shown in Figure 14 above, which will cause clogging in the chiller pipes.

This balance resulted in an achieved COP of 0.72 being slightly above average for commercial LiBr-H_2O single effect absorption chiller COP normally in the range of 0.65 to 0.85 [67, 68]. Table 8 below presents these results.

Table 8. Single effect LiBr-H_20 absorption chiller external stream inlet temperatures, component duty, pump work and COP results from ASPEN PLUS.

	Temperature in (°C)	Temperature out (°C)	Duty (MW)
Condenser	25	32.38	2.46
Absorber	25	34.25	3.08
Desorber	85	75.17	3.21
Evaporator	15	7.01	2.33
Pump Work (W)	84		
COP	0.72		

5.2.7 Plant monthly energy utilization improvement in warmer months

Table 2 and Table 5 presented the calculated thermal energy recovered from the district heating supply stream for the chiller system to have the values of $1.9865*10^4$ kJ/s and $1.5892*10^4$ kJ/s for the recommended operational parameters at set point temperatures 90°C and 80°C respectively. Also, Table 6 presented the calculated thermal energy recovered from the condensate stream for additional heating to have a value of $3.8056*10^3$ kJ/s at set point temperature 80°C.

The energy recovered by the chiller stream from the district heating supply stream is categorized under the district heating energy consumption given it originates from that stream. While the energy recovered by the chiller stream from the condensate stream for additional heating is not categorized under the district heating energy consumption given it does not

originate from that stream. It is rather categorized separately as part of the plant total energy consumption.

The chiller system energy utilization values presented in kJ/s above have the following conversions to MW:

$1.9865*10^4$ kJ/s = 19.865 MW for set point temperature 90°C from district heating stream

$1.5892*10^4$ kJ/s = 15.892 MW for set point temperature 80°C from district heating stream

$3.8056*10^3$ kJ/s = 3.8056 MW for set point temperature 80°C from condensate stream

In order to convert the chiller system thermal energy utilization from MW to MWh, the monthly operational hours of the chiller are required. Assuming the chiller will be in operation 24 hours per day during the warmer months of the year from May – September, the monthly operational hours will be either 720 h or 744 h for the months with 30 and 31 days respectively. Also, given the specific set point temperature at which the plant will operate during the warmer months is dependent on ambient temperature and heating demand in the district heating network and can be either 80°C, or 90°C, it is not possible to determine exactly which months the plant will be operated at a set point temperature of 80°C, or 90°C. This affects which chiller system monthly energy utilization value presented in MW above will be used for a 30 day or 31 day per month calculation.

It is therefore assumed that the monthly operational hours of the chiller are 744 h for all warmer months of May – September.

5.2.7.1 District heating monthly energy utilization for warmer months with proposed system at set point temperature 90°C

The district heating monthly average energy utilization for the warmer months from section 4.3 was mentioned to be 4258 MWh for Returkraft´s system with efficiency drawbacks presented in this study.

The district heating monthly energy utilization in MWh for the proposed system at the set point temperature of 90°C during the warmer months of May – September is given by:

District heating energy utilization for the warmer months with proposed system (90°C) =

Chiller system monthly energy utilization (90°C) + District heating monthly average energy utilization in warmer months for efficiency drawback system

= (19.865 MW * 744 h) + 4258 MWh

= 19 037.56 MWh

5.2.7.2 District heating monthly energy utilization for warmer months with proposed system at set point temperature 80°C

The district heating monthly energy utilization in MWh for the proposed system at the set point temperature of 80°C during the warmer months of May – September is given by:

District heating monthly energy utilization for the warmer months with proposed system (80°C) =

Chiller system monthly energy utilization (80°C) + District heating monthly average energy utilization in warmer months for efficiency drawback system

= (15.892 MW * 744 h) + 4258 MWh

= 16 081.64 MWh

5.2.7.3 Average plant monthly energy utilization improvement for warmer months

In order to calculate the plant´s monthly energy utilization improvement for the warmer months, an average of both district heating monthly energy utilization values with proposed system for set point temperatures 90°C and 80°C obtained in sections 5.2.7.1 and 5.2.7.2 respectively will first need to be calculated.

Average district heating monthly energy utilization for the warmer months with proposed system =

$$\frac{19\,037.56\ \text{MWh} + 16\,081.64\ \text{MWh}}{2} = 17\,559.6\ \text{MWh}$$

The monthly average total energy produced by the plant from waste incineration was mentioned in section 4.3 to be 29 274 MWh, and the monthly average energy utilization for electricity production through the steam turbine was mentioned also in section 4.3 to be 7 424 MWh.

The plant´s monthly total energy consumed in the warmer months is given by:

Plant monthly total energy consumed in warmer months =

Average district heating monthly energy utilization for the warmer months with proposed system + Steam turbine monthly average energy utilization in warmer months + Chiller system monthly energy utilization (Condensate stream)

= 17 559.6 MWh + 7 424 MWh + (3.8056 MW * 744 h)

= 27 814.97 MWh

The average plant monthly energy utilization improvement for the warmer months is given by:

$$\frac{\text{Plant monthly total energy consumed in warmer months}}{\text{Monthly average total energy produced by the plant}} * 100$$

=

$$= \frac{27\ 814.97\ \text{MWh}}{29\ 274\ \text{MWh}} * 100 \approx 95\%$$

This presents an average plant monthly energy utilization improvement for the warmer months of May – September from 41% mentioned in section 4.3 to now about 95% with the proposed system.

5.2.8 Economic analysis

A basic economic analysis was conducted to provide some entirety to this study. The investment cost to the proposed system was estimated, together with the return on investment time.

5.2.8.1 Investment cost

Three separate absorption chiller suppliers (Table 9) were contacted for pricing information based on the waste heat fluid temperature and flow rate, and the desired cooling load. The waste heat fluid in this case was water which had a temperature of 85°C. The ASPEN PLUS simulation calculated a cooling load of 2.33 MW as was presented in Table 8 above.

Also, several piping suppliers were contacted for pricing information on the cost of piping for the river water source which is at a direct distance of 1.30 km from the plant as illustrated in Figure 26. Only one supplier (Table 10) responded and therefore was the only price presented. A piping length of 2 km was used in this case taking into consideration any unforeseen rerouting

of the pipes due to physical obstacles in the area. The pricing was provided in a range, given there were several aspects such as; soil type, need for X-ray tomography, number of bends required and the type of insulation which needed to be taken into consideration in order to get an exact price. Thus, an average of this range was used in the price estimation. The price range also included DN300 pipes equivalent to about 30 cm in diameter district cooling insulated supply and return pipes buried 1 m underground.

In addition to this, the pricing of heat exchangers: HX1, HX2, HX3 and HX4 presented in chapter 5.2.3 and 5.2.4 were obtained from a heat exchanger supplier (Table 11). The 80°C and 90°C set point temperatures provided two different values for the required heat transfer area of HX3. In this situation, the larger heat transfer area was prioritized given it guarantees adequate heat transfer during operation at both set point temperatures.

The investment costs of the pumps were excluded given the need of a separate analysis required to determine the number of pumps needed. This analysis will require the total length of the pipes including bends required to setup the installation. Which in turn will be based on the exact location of the chiller on Returkraft´s property and the complexity of the piping.

Costs regarding operation and maintenance were only limited to the maintenance cost of the chiller. This was so given some vital decisions are yet to be made such as: type of pumps, required number of pumps, size of pumps and length of pipes. Knowing these would provide information necessary to estimate the complete operations and maintenance costs of the cooling plant.

Table 9. 2 MW single effect LiBr-H_20 absorption chiller suppliers, models and prices

Supplier	Chiller Model	Cooling Capacity (MW)	Unit Price (NOK)
Thermax Europe Ltd	RECO AQUA (TAC L5 F3)	2	2 600 000
Dalian BingShan Refrigeration	PANASONIC (LLC-102DH)	2	3 650 000
Teknotherm AS	HEINAN & HOPMAN (HWAR-L1125HH)	2	6 289 000

Table 10. Pricing information for DN300 insulated district cooling pipes and installation.

Supplier	Insulated Pipe Size	Price range per meter (NOK)	Average price per meter (NOK)	Total price for 2 km (NOK)
VVS Gruppen AS	DN300	6000 - 9000	7500	15 000 000

Table 11. Supplier, model, heat transfer area, and pricing information for HX1, HX2, HX3, and HX4.

Supplier	Heat Exchanger Model	Heat Exchanger Name	Heat Transfer Area (m^2)	Unit Price (NOK)
Hofmann Engineering Technology Ltd	ALFA LAVAL PHE T20B-365PCS	HX3	284	135 000
Hofmann Engineering Technology Ltd	ALFA LAVAL PHE T20B-276PCS	HX4	230	103 500
Hofmann Engineering Technology Ltd	ALFA LAVAL PHE M15B-336PCS	HX2	170	74 000
Hofmann Engineering Technology Ltd	ALFA LAVAL PHE M15B-189PCS	HX1	88	43 700
				Total sum = 356 200

Given the PANASONIC (LLC-102DH) chiller is chosen, the total investment cost for the proposed cooling system will be given by:

Total Investment Cost = Chiller Cost + Piping Cost + Heat Exchanger Cost

= 3 650 000 kr + 15 000 000 kr + 356 200 = 19 006 200 (NOK) kr

5.2.8.2 Income stream

In order to calculate the payback time, an income stream had to be established in the first place. Income streams usually are in the form of financial savings or payments from supplied services. When it comes to savings option, savings on electricity bills were not considered. This is because the electricity consumption from the condenser fans in the glycol cycle which went to cooling the district heating water return stream, could not be compared yet to the electricity

costs of operating the pumps in the proposed system. This is due to the lack of information on the pumps at this point in time as mentioned earlier in section 5.2.8.1. Thus, the income stream was based solely on payments from supplied services.

In order to establish a correct pricing base for the sale of cooling services, the prices of Lyse AS, Stavanger [69] were used to estimate the yearly income from selling all 2 MW of cooling produced. Also, the sale of cooling services was limited the warmer months of the year from May – September. The pricing table is presented below with all prices in NOK and excluding VAT (Value Added Tax).

Table 12 below mentions NordPool Day-ahead prices which are prices for electricity on an electricity market. This electricity market is used by power producers and buyers in the Nordic areas for trading with one another. The transactions take place on "a day-ahead" principle where electricity is traded a day ahead to help balance supply and demand of electricity [70]. These prices are usually reflected by electricity providers on their clients, and if the clients are companies, they usually in turn reflect these costs on the sales prices of their services so as to cover electricity costs associated with production which is the case here with Lyse AS. Given this, the income from the NordPool Day-ahead prices will not be taken into consideration since the operating costs for the pumps which are the main electricity consumers in the proposed system have not been considered.

Table 12. Pricing table for district cooling from Lyse AS.

Cooling with ordered load:	Under 200 kW	Over 200 kW
Monthly fee	129 kr (NOK)	3200 kr (NOK)
Base fee	21 cents (NOK)/ kWh	21 cents (NOK)/ kWh
NordPool Day-ahead prices	x cents (NOK)/ kWh	x cents (NOK)/ kWh
Ordered cooling load	659 kr (NOK)/kW/year	470 kr (NOK)/kW/year

- **Calculations**

Both cases of "Under 200 kW" and "Over 200 kW" which were presented in Table 12 above, will be calculated below.

- **Under 200 kW**

For the case of “Under 200 kW”, an ideal situation is considered whereby 20 clients are assumed to be purchasing 100 kW of cooling each monthly.

1 NOK cent = 0.01 kr => 21 NOK cent = 0.21 kr

Months that require cooling: May-September

Number of months/year that require cooling = 5

Amount of cooling produced/year = 2000 kW * 5 = 10 000 kW

Number of operating hours/year = Σ No days for each month * 24 h

= 3672 h

Yearly fee per client: 129 kr * 5 = 645 kr

Yearly fee for all clients: 645 kr * 20 = 12 900 kr

Base fee all clients per year: 0.21 kr/kWh * 10 000 kW * 3672 h = 7 771 200 kr

Ordered cooling load per year all clients: 659 kr/kW/year * 10 000 kW/year = 6 590 000 kr

Total Income/year all clients: Yearly fee for all clients + Base fee all clients per year + Ordered cooling load per year all clients

= 12 900 kr + 7 771 200 kr + 6 590 000 kr

= 14 314 100 (NOK) kr

- **Over 200 kW**

The same calculations above is repeated, only the rates which are changed to “Over 200 kW” rates and an ideal situation is considered whereby 5 clients are assumed to be purchasing 400 kW of cooling each monthly.

Yearly fee per client: 3 200 kr * 5 = 16 000 kr

Yearly fee for all clients: 16 000 kr * 5 = 80 000 kr

Base fee all clients per year: 0.21 kr/kWh * 10 000 kW * 3672 h = 7 771 200 kr

Ordered cooling load per year all clients: 470 kr/kW/year * 10 000 kW/year = 4 700 000 kr

Total Income/year all clients:

= 80 000 kr + 7 771 200 kr + 4 700 000 kr

= 12 491 200 (NOK) kr

5.2.8.3 Payback time

Given the yearly income has been calculated, all other yearly expenditures incurred to the cooling production system will normally have to be subtracted from the yearly income. One of such expenditures is the yearly maintenance cost of the chiller. In a study carried out by Zabala E.S, the maintenance cost of an absorption chiller was concluded to be very low due to the lack of moving machinery and therefore few components that demand maintenance which is mainly cleaning; thus costs can be neglected [71].

$$Payback\ Time\ = \frac{Total\ Investment\ Cost}{Total\ yearly\ Income} \qquad (5\text{-}1)$$

$$Payback\ time\ (Under\ 200\ kW) = \frac{19\ 006\ 200\ (\text{NOK})\text{kr}}{14\ 314\ 100\ (\text{NOK})\text{kr}} = 1.3\ yr$$

$$Payback\ time\ (Over\ 200\ kW) = \frac{19\ 006\ 200\ (\text{NOK})\ \text{kr}}{12\ 491\ 200\ (\text{NOK})\ \text{kr}} = 1.5\ yr$$

The payback time presented above is for an ideal situation where all 10 000 kW of cooling are purchased by clients and consumed. Several other factors not taken into consideration such as: prices of the pumps, chiller installation costs, production stoppages, and eventual repair costs, will all contribute to extending the payback time. Moreover, the actual amount of cooling being sold yearly will also have a considerable impact on the payback time. Given all of these, the actual payback time of the proposed system will be higher than what is presented above.

5.2.9 Environmental analysis

Environmental analysis in this case is the process of examining the environmental impacts of the proposed system prior to the decision-making process to move forward with the implementation of the system.

5.2.9.1 Sustainable development and power demand

The Paris Agreement of 2015 [72] on holding the global temperatures below 2°C and pursuing efforts to limiting it to 1.5°C, demands sharp carbon emission cuts and technologies providing efficient and cost effective energy in order to deal with the impacts of climate change.

Having LiBr-H_2O as the chiller working refrigerant pair does not contribute to climate change. The refrigerant pair is non-flammable and non-toxic. In addition, it has no associated environmental hazards, Ozone Depletion Potential (ODP), nor Global Warming Potential (GWP).

With an ever growing society and the digitalization of these societies, dependency on electricity has never been greater. This growth has contributed to an increase in global electricity demand of 4% in 2018 [73], of which power grids need to meet up with. Meeting the peaks in demand is one of the reasons for increased emissions from electricity generation given peak electricity demands usually are met by fossil fuel generations [74].

Given this, the production of cooling from waste or “free” heat, takes away the peak power demand on the electrical grid which could otherwise have been inflicted by individual electricity-powered cooling units resulting in increased emissions. Making use of the already existing thermal energy is sustainable and increases the overall efficiency of the plant.

6 Conclusion

Waste incineration is a better method for waste management than landfilling since it can reduce pollution and additionally create value such as electricity and heating. However, the energy efficiency drawbacks in waste incineration plants in Norway coupled with the lack of a similar study within this subject for Norway inspired the need to conduct this study.

With acquired data from Returkraft AS, it was discovered during the analysis that for each month, about 10 836 MWh of thermal energy was being cooled to ambient air and wasted during the warmer months (May-September). It was noticed that the energy being wasted, was primarily as a result of cooling the district heating return water stream using high temperature water from the supply stream. An alternative system is suggested for implementation in order to minimize the wasted thermal energy.

The system suggests using a heat exchanger (HX3) at a 90°C set point temperature to recover thermal energy from the branched out district heating supply water stream. This results in the stream being cooled down and introduced to the district heating return water stream to reduce its temperature. At a set point temperature of 80°C, an additional heat exchanger (HX4) is introduced using condensate in order to achieve the desired chiller drive water temperature of 85°C.

The thermal energy transfer across the fluids in the heat exchangers is calculated and the required heat transfer areas for the heat exchangers are determined. In addition, an absorption chiller model is built and simulations are carried out on ASPEN PLUS in order to assess the amount of cooling which could be produced with the recovered thermal energy. The simulations show that 2.33 MW of cooling could be achieved, producing a chill water temperature of 7.01°C. The proposed system also improves the energy utilization of the plant during the warmer months of May – September from 41% to about 95%.

Moreover, the possibility of using river water to cool the chiller desorber water, the absorber cooling water and condenser cooling water is considered. Water from the river in question (river Otra) being at a direct distance of 1.30 km from Returkraft´s plant is pumped to the plant. Two heat exchangers (HX1, HX2) are used to carry out the cooling.

Furthermore, an economic analysis is carried out to provide an estimate of the costs of investing in the proposed system and the payback time. The total investment cost is 19 006 200 NOK,

not taking into consideration the chiller installation costs and the purchase cost of the pumps. Using the rates from Lyse AS for district cooling, a yearly income estimate is calculated assuming all 10 000 kW of cooling produced yearly get sold to 20 clients purchasing 100 kW of cooling monthly and 5 clients purchasing 400 kW of cooling monthly. This shows a yearly income of 14 314 100 NOK and 12 491 200 NOK with a payback time of 1.3 and 1.5 years respectively for both cases.

Finally, an environmental analysis is made which highlights the reduction in emissions by producing cooling using waste thermal energy. The LiBr-H_2O refrigerant pair is also presented to be non-toxic, non-flammable and has no associated environmental hazards, ODP, nor GWP.

The results from this study shows that recovery of waste heat is essential and its use for cooling is practical with increasing global temperatures. Nonetheless, the investment costs are high and the payback time could be much longer than estimated. However, the benefits of waste heat recovery are massive with a wide variety of applications available, thus making the investment worthwhile long-term. The waste incineration industry in Norway has come far since its implementation and still has room for progress with regards to thermal energy efficiency.

7 Recommendations for future work

- Finding alternative methods for cooling the district heating return water stream. The proposed system in this study suggests the use of a heat exchanger in order to recover thermal energy from the branched out district heating supply water stream. This results in the stream being cooled down in order to reduce the district heating return water stream. Finding alternative methods of cooling the district heating return water stream will provide an opportunity for the branched out hot water stream to drive the chiller directly without the need for a heat exchanger.
- Due to time constraints, an analysis on the number and size of pumps required for the proposed system could not be done. Carrying out this analysis will provide more accuracy to the economic analysis conducted in this study.
- Study heat recovery from exhaust gases after the boiler. The exhaust gases when leaving the boiler still contain a lot or thermal energy which get cooled down at the different gas cleaning stages. Studying the feasibility of energy recovery from that source could contribute to minimizing waste heat even further.
- This study proposed the use of the waste thermal energy for cooling purposes. Options such as thermal energy storage can be considered for peak load use on the coldest winter days.

8 References

1. Norge, A. *Deponi*. 2020; Available from: https://www.avfallnorge.no/hva-jobber-vi-med/fagomr%C3%A5der/deponi.
2. B. B Patil, A.A.P., A. A Kulkarni, *Waste to Energy by Incineration*, in *Environmental Science and Technology Department*. 2014, Shivaji University, Kolhapur India.
3. Norge, A. *Energiutnyttelse*. 2017 [cited 2020 12.04.20]; Available from: http://kurs.avfallnorge.no/energiutnyttelse1.cfm.
4. Hartmann, D.L., *Observations: Atmosphere and Surface*. 2013.
5. IPCC, *Contribution of Working Group I to the Fourth Assessment Report of the Intergovernmental Panel on Climate Change*, S. Solomon, Editor. 2007.
6. Sonia I. Seneviratne, M.G.D., Brigitte Mueller & Lisa V. Alexander, *No pause in the increase of hot temperature extremes*. 2014.
7. Norway, M.o.t.E.o., *Norway´s Fifth National Report under the United Nation´s Framwork Convention on Climate Change.* 2009.
8. J.O Gjershaug, G.M.R., S. Öberg, M. Qvenild, *Alien Species and Climate Change in Norway. An assessment of the risk of spread due to global warming* 2009.
9. Shakerin, M., *Analysis of district heating systems integrating distributed sources*, in *Department of Energy and Process Engineering*. 2017, Norwegian University of Science and Technology. p. 113.
10. Jinggang Wang, X.G., *The Study of Cooling Water Waste Heat Recovery in Chemical Plant by Heat Pump System*. 2010.
11. Dominković, D.F., *Potential of district cooling in hot and humid climates*. 2017.
12. Satish Maurya, D.P., *Combined Refrigeration Cycle for Thermal Power Plant Using Low Grade Waste Steam*. 2014.
13. Chien-Yeh Hsu, T.-Y.L., Jyun-De Liang, Ching-Hsien Lai, Sih-Li Chen, *Optimization analysis of waste heat recovery district cooling system on a remote island: Case study Green Island*. 2019.
14. Kommune, O., *Avfallets historie: produksjon og håndtering av avfall gjennom tidene*. 2020.
15. Kommune, O. *Haraldrud sorteringsanlegg*. 2020 20.04.20]; Available from: https://www.oslo.kommune.no/avfall-og-gjenvinning/haraldrud-sorteringsanlegg/.
16. (HRA), H.o.R.A.A. *HRAs historie*. 2020 20.04.20]; Available from: https://hra.no/om-hra/hras-historie/.
17. Miljødirektoratet, M. *Avfallforbrenning med energiutnyttelse*. 2019 23.04.20]; Available from: https://miljostatus.miljodirektoratet.no/tema/avfall/avfallshandtering/avfallsforbrenning-med-energiutnyttelse/.
18. Varme, F. *Fakta om Fortum Oslo Varmes anlegg på Klemetsrud*. 2020 23.04.20]; Available from: https://www.fortum.no/bedrift-og-borettslag/avfall-og-energigjenvinning/vare-forbrenningstjenester/fakta-om-fortum-oslo-varmes-anlegg-pa-klemetsrud.
19. BIR. *Om energianlegget* 2020 23.04.20]; Available from: https://bir.no/avfallsforbrenning/om-energianlegget/.
20. Statkraft. *Trondheim fjernvarme*. 2020; Available from: https://www.statkraft.no/Energikilder/vaare-kraftverk/norge/trondheim-fjernvarme/.
21. Returkraft. *Om Returkraft*. 2020 23.04.20]; Available from: https://www.returkraft.no/om-returkraft.
22. Energigjenvinning, F. *Om Forus Energigjenvinning* 2020 23.04.20]; Available from: http://forusenergi.no/om-oss.

23. KF, F. *Energigjenvinningsanlegg* 2020 23.04.20]; Available from: http://www.frevar.no/vare-anlegg/energigjenvinningsanlegg/.
24. Energi, Ø. *Fjernvarme og energigjenvinning* 2020 23.04.20]; Available from: https://www.ostfoldenergi.no/energikilder/fjernvarme/mer-om-fjernvarme/.
25. Borregaard. *Nytt energigjenvinningsanlegg reduserer oljeforbruket ved Borregaard fabrikker med 20 000 tonn*. 2020 23.04.20]; Available from: https://www.borregaard.no/Nyheter/Nytt-energigjenvinningsanlegg-reduserer-oljeforbruket-ved-Borregaard-Fabrikker-med-ca-20-000-tonn.
26. Kraft, T. *Naturlig nav: Grautneset*. 2020 23.04.20]; Available from: https://www.tafjord.no/konsern/energigjenvinning/naturlig-nav/.
27. Varme, K. *Skattøra Varmesentral*. 2020 23.04.20]; Available from: https://kvitebjornvarme.no/skattora/category890.html.
28. Norge, A. *Kart over bransjen*. 2020 23.04.20]; Available from: https://www.avfallnorge.no/om-avfall-norge/om-bransjen.
29. Miljødirektoratet. *Evaluering av bortfall av forbrenningsavgiften på avfall*. 2014 23.04.20]; Available from: http://tema.miljodirektoratet.no/Documents/Nyhetsdokumenter/Evaluering%20av%20bortfall%20av%20forbrenningsavgift%20p%C3%A5%20avfall%20Mepex.pdf.
30. Bioenergi, E. *Eidsiva Bioenergi*. 2020 23.04.20]; Available from: https://www.eidsiva.no/om-eidsiva/selskapene/.
31. IKS, S.A. *Senja Avfall IKS*. 2020 23.04.20]; Available from: https://www.senja-avfall.no/no/senja-avfall-iks.
32. Renovasjon, H. *Om Hallingdal Renovasjon*. 2020 23.04.20]; Available from: https://www.hallingdalrenovasjon.no/om-oss/.
33. Daimyo. *Kvitebjørn Bio-EL*. 2020 23.04.20]; Available from: https://www.daimyo.no/kvitebjornbioel-eng.
34. Kommune, Å. *Geithus forbrenningsanlegg*. 2020 23.04.20]; Available from: https://www.ardal.kommune.no/geithus-forbrenningsanlegg.6280165-155525.html.
35. Garud R. M, S.K., Kore V. S, Kulkarni G. S, *A Short Review on Process and Applications of Reverse Osmosis* 2011.
36. Emis. *Fabric filter*. 2020 [cited 2020; Available from: https://emis.vito.be/en/bat/tools-overview/sheets/fabric-filter.
37. Leksikon, S.N. *Elektrofilter*. 2018 [cited 2020; Available from: https://snl.no/elektrofilter.
38. Fortum. *Røykgassrensing trinn for trinn*. 2020 [cited 2020; Available from: https://www.fortum.no/bedrift-og-borettslag/avfall-og-energigjenvinning/vare-forbrenningstjenester/fakta-om-roykgassrensing.
39. Sambo A. Umar, A.Y.B., Momoh Jimoh, Esther Salami, Raisuddin Khan, *Control of particulate matter (PM) emissions from industrial plant using anfis based controller*. 2016.
40. Vølund, B.W. *Sundsvall Energi in Sweden*. 2020; Available from: http://www.volund.dk/References_and_cases/Waste_to_energy_solutions/Sundsvall.
41. Delangle, A.C.C., *Modelling and optimisation of a district heating network´s marginal extension*. 2016, Imperical College London London.
42. A.I. Fernandez, C.B., L. Miro, S. Bruckner, L.F. Cabeza, *Thermal energy storage (TES) systems using heat from waste*. 2015.
43. Alfalaval. *The theory behind heat transfer*. 2004 [cited 2020 22.06.20]; Available from: https://www.alfalaval.com/globalassets/documents/microsites/heating-and-cooling-hub/alfa_laval_heating_and_cooling_hub_the_theory_behind_heat_transfer.pdf.

44. DHCS, K. *Keppel DHCS District Cooling System*. 2020 [cited 2020 11.05.20]; Available from: http://www.keppeldhcs.com.sg/our_product_overview.html.
45. McKinney, W., *Python Pandas version 1.0.3 (2020). Wes McKinney*. 2020.
46. Hunter, J.D., *Matplotlib version 3.2.1 (2020) John D. Hunter*. 2020.
47. Rossum, G.v., *Python version 3.8.2 (2020) Guido van Rossum* 2020.
48. Inc, T.M., *Matlab version 9.6 (R2019a). Natick, Massachusetts: The MathWorks Inc; 2019*. 2019.
49. Inc, A.T., *Aspen Plus version 9.0 (2016). Bedford, Massachusetts: Aspen Technology Inc*. 2016.
50. Alder, G., *DRAW.IO (2020) Gaudenz Alder*. 2020.
51. Somers, C., *Simulation of Absorption Cycles for Integration into Refining Process*. 2009, University of Maryland.
52. Georgios A. Florides, S.A.K., *Optimisation and cost analysis of a lithium bromide absorption solar cooling system* 2007.
53. Salem M. Osta-Omar, C.M., *Mathematical Model of a Lithium-Bromide/Water Absorption Refrigeration System Equipped with an Adiabatic Absorber*. 2016, University of Malta.
54. Lawan, S., *Thermodynics analysis of a single and series flow double effect solar assisted absorption refrigeration system using LiBr-H2O working pairs* 2017, Cyprus International University
55. Lawan, S., *Thermodynamic analysis of single and series flow double effect solar assisted absorption refrigeration systems using LiBr-H2O working pairs.* , in *Energy Systems Engineering Department*. 2017, Cyprus International University p. 87.
56. Welch, T., *Module 10: Absorption refrigeration.* CIBSE JOURNAL, 2009.
57. Young-Hoon Kwak, D.-S.K., Se-Hwan Cheon, Ro-Yeul Kwak, Jung-Ho Huh, *Condensing Temperature Control through Energy Management Simulation for Large Office Building*, in *Department of Architectural Engineering*. 2011, University of Seoul, Korea.
58. AS, R. *Hvordan virker anlegget?* 2019 [cited 2020; Available from: https://assets.website-files.com/5aa0076038aaa40001cf75b0/5cd135e1e4929d85a34b5eac_Faktaark%20_Hvordan%20virker%20anlegget.pdf.
59. Comission, E. *Energy performance of buildings directive*. 2020 26.05.20]; Available from: https://ec.europa.eu/energy/topics/energy-efficiency/energy-efficient-buildings/energy-performance-buildings-directive_en.
60. Vegge, T.F., *Halvparten av energien blir ikke utnyttet.* Fædrelandsvennen 2015.
61. AS, R. *Returkraft Timelaps av byggeprosessen*. 2020 [cited 2020; Available from: https://www.youtube.com/watch?v=LGPJv78eyxE.
62. Ragnar Heggstad, G.T., *Otra.* Store Norske Leksikon (SNL), 2020.
63. Norway, V., *Otra.* Visit Norway, 2020.
64. AS, O.V., *Teknisk bestemmelser for tilkobling til fjernkjølenettet* 2015. p. 15.
65. Jangsten, M., *High Temperature District Cooling- Possibilities and challenges based on an existing system and its connceted buildings*. 2019, Chalmers University of Trechnology, Gothenburg Sweden.
66. Ludwig, E.E., *Applied Process Design for Chemical and Petrochemical Plants*. Vol. 3. 2001, Boston, Oxford, Auckland, Johannesburg, Melbourne, New Delhi: Gulf Professional Publishing.
67. Molter, F., *Solar Next Chillii Cooling Kit*. 2019. p. 48.
68. Max Santini, T.D., *Module 91: High efficiency heat-powered lithium bromide absorption chillers* CIBSE JOURNAL, 2016.

69. AS, L. *Pris for Kjøling*. 2020; Available from: https://www.lyse.no/varme/priser.
70. Pool, N. *About us*. 2020; Available from: https://www.nordpoolgroup.com/About-us/.
71. Zabala, E.S., *Technological and Economic Evaluation of District Cooling with Absorption Cooling Systems in Gavle (Sweden)*, in *Department of Technology and Built Environment* 2009, University of Gavle. p. 178.
72. Commision, E. *Paris Agreement*. 2020; Available from: https://ec.europa.eu/clima/policies/international/negotiations/paris_en.
73. (IEA), I.E.A. *Global energy demand rose by 2.3% in 2018, its fastest pace in the last decade*. 2019; Available from: https://www.iea.org/news/global-energy-demand-rose-by-23-in-2018-its-fastest-pace-in-the-last-decade.
74. Khan, I., *Energy-saving behaviour as a demand-side management strategy in the developing world: the case of Bangladesh.* Springer Link, 2019.

9 Appendices

Appendix A

Heat exchanger calculations script written in MATLAB R2019a

```
%Heat transfer across two fluids
%Hot side fluid properties
T_Hot_In =  90;
T_Hot_Out = 76;
m_Hot = 65;
Cp = 4.182;
Delta_T_Hot = minus (T_Hot_Out, T_Hot_In);
%Q_Hot = m_Hot * Cp * Delta_T_Hot
X1 = times (m_Hot,Cp);
Q_Hot = times (Delta_T_Hot, X1);

%Cold side fluid properties

%The heat removed from the hot stream is equal in magnitude to the heat
%absorbed by the cold stream. Q_Hot = Q_Cold
T_Cold_In = 73.7;
m_Cold = 78;
Q_Cold = -(Q_Hot);
X2 = times (m_Cold,Cp)
Y1 = rdivide (Q_Cold, X2);
T_Cold_Out = plus (Y1, T_Cold_In);

%Heat exchanger area
%Q = U * A * Delta_T_LMTD
%Delta_T_LMTD = (Delta_T_B - Delta_T_A)/ Ln(Delta_T_B / Delta_T_A)
%Delta_T_B = T_Hot_In - T_Cold_Out
%Delta_T_A = T_Hot_Out - T_Cold_In
Delta_T_B = minus(T_Hot_In, T_Cold_Out);
Delta_T_A = minus(T_Hot_Out, T_Cold_In);
Z1 = minus (Delta_T_B, Delta_T_A);
Z2 = rdivide (Delta_T_B, Delta_T_A);
Z3 = log (Z2);

Delta_T_LMTD = rdivide (Z1, Z3);

%U is the Overall heat transfer coefficient
%An assumption is made for the value of U for liquid to liquid fluids
%Q_Cold has the units KJ/s and is converted to J/s and prsented as Q
%Required heat exchanger area (A) is presented in m^2
U = 6750;
Z4 = times (U, Delta_T_LMTD);
Q = times (Q_Cold, 1000);
A = rdivide (Q, Z4);
```

Appendix B

This script reads the Flakksvann water temperature data for every half-hour from June 2019 to June 2020 obtained from the NVE. When the data was imported, it was unstructured and therefore had to be filtered to obtain the desired structure of two columns with the temperature and date/time. The monthly average temperature is calculated and plotted as shown in Figure 27.

```
import pandas as pd
import numpy as np
from pandas import read_csv
import csv
from csv import reader
import datetime as dtm
from datetime import datetime, timedelta
import seaborn as sns
sns.set()
import time
import matplotlib.pyplot as plt
plt.rcParams.update({'figure.max_open_warning': 0})
import matplotlib.dates as mdates
import os
np.warnings.filterwarnings('ignore')
#pylint: disable=no-member
from PIL import Image

crt_yr = dtm.datetime.utcnow().year
crt_month = dtm.datetime.utcnow().month
crt_day =dtm.datetime.utcnow().day
crt_time = dtm.datetime.utcnow().replace(microsecond=0)
crt_hour = crt_time.hour
crt_minute = crt_time.minute
end_range = crt_time

start_time = dtm.datetime(year=2019, month=5, day=31)
end_time = dtm.datetime(year=2020, month=6, day=1)

sns.set_style("whitegrid")

df = pd.read_csv('Flakksvann_temp.csv',sep= " ")
df.columns = ['Date', 'Time', 'No', 'Nope', 'Nei', 'Nada', 'Some', 'Data']

df['temp1'] = df['Some'].combine_first(df['Data'])
df['temp2'] = df['No'].combine_first(df['Nei'])
df['temp3'] = df['Nope'].combine_first(df['Nada'])
df['temp4'] = df['temp1'].combine_first(df['temp2'])
df['temp'] = df['temp4'].combine_first(df['temp3'])

df.drop(['No', 'Nope', 'Nei', 'Nada', 'Some', 'Data', 'temp1', 'temp2', 'temp3', 'temp4'], axis = 1, inplace = True)
df['Time'] = df['Time'].astype(str)
df['Date'] = df['Date'].astype(str)
df['Time'] = df['Time'].str.replace(';', '')


df['timestamp'] = pd.to_datetime(df['Date'] + ' ' + df['Time'])
df.drop(['Date', 'Time'], axis=1, inplace=True)
df.set_index('timestamp', inplace=True)

df_month = df['temp'].resample('M').mean()
df_month.to_csv('mean.csv', sep=" ")

df = pd.read_csv('mean.csv', sep=" ")
df['timestamp'] = pd.to_datetime(df['timestamp'], format = '%Y-%m-%d')
df.set_index('timestamp', inplace=True)

df = df['2019-05-31':'2020-06-30']


fig, ax = plt.subplots(figsize=(15,7))
ax.plot(df.index, df.temp.values)

ax.xaxis.set_major_locator(mdates.MonthLocator(interval=1))
ax.xaxis.set_major_formatter(mdates.DateFormatter('%b %Y'))
ax.set_xlim(left=start_time, right=end_time)
```

Appendix C

This script produces Figure 23. The input data used to plot the graph was Returkraft´s monthly district heating thermal energy data for the years 2017, 2018, and 2019 read from an excel file. The data was plotted, and personal user styling preference was inputted.

```
import pandas as pd
import numpy as np
import datetime as dtm
from datetime import datetime, timedelta
import seaborn as sns
import time
import matplotlib.pyplot as plt
import matplotlib.dates as mdates

crt_yr = dtm.datetime.utcnow().year
crt_month = dtm.datetime.utcnow().month
crt_day =dtm.datetime.utcnow().day
crt_time = dtm.datetime.utcnow().replace(microsecond=0)
crt_hour = crt_time.hour
crt_minute = crt_time.minute
end_range = crt_time

start_time = dtm.datetime(year=2019, month=1, day=1, hour=0, minute=0)
end_time = dtm.datetime(year=2019, month=12, day=1, hour=0, minute=0)

df = pd.read_excel("district_heating.xlsx", sep=" ")

df.columns = ['Time', 'year_1', 'year_2', 'year_3']

df.set_index('Time', inplace=True)

sns.set_style("white")
sns.set(style="ticks", context="talk")


fig, ax = plt.subplots(figsize=(15,9))

ax.grid(False)


ax.plot(df.index, df.year_1.values, label='2017', marker='o')
ax.plot(df.index, df.year_2.values, label='2018', marker='s')
ax.plot(df.index, df.year_3.values, label='2019', marker='v')

plt.gca().legend(loc='upper right', bbox_to_anchor=(1.13, 1.02))

ax.set_xlim(left='Jan', right='Dec')
plt.xticks(rotation = 45)

ax.set_xlabel('Time (Months)', fontsize=16, fontweight="bold")
ax.set_ylabel('Energy (MWh)', fontsize=16, fontweight="bold")
ax.set_title('District Heating', fontsize=18, fontweight="bold")

plt.savefig('district_heating_combined.png', dpi=300)
```

Appendix D

This script reads Returkraft´s monthly thermal energy utilization data (percentage) and the monthly waste burn data (tons) for the years 2017, 2018, and 2019. The monthly thermal energy utilization data and the monthly waste burn data are represented in Figure 20 and Figure 19 respectively.

```
import pandas as pd
import numpy as np
import datetime as dtm
from datetime import datetime, timedelta
import seaborn as sns
import time
import matplotlib.pyplot as plt
import matplotlib.dates as mdates

crt_yr = dtm.datetime.utcnow().year
crt_month = dtm.datetime.utcnow().month
crt_day =dtm.datetime.utcnow().day
crt_time = dtm.datetime.utcnow().replace(microsecond=0)
crt_hour = crt_time.hour
crt_minute = crt_time.minute
end_range = crt_time

start_time = dtm.datetime(year=2019, month=1, day=1, hour=0, minute=0)
end_time = dtm.datetime(year=2019, month=12, day=1, hour=0, minute=0)

df = pd.read_excel("energy_utilization.xlsx", sep=" ")

df.columns = ['Time', 'year_1', 'year_2', 'year_3']

df.set_index('Time', inplace=True)

sns.set_style("white")
sns.set(style="ticks", context="talk")

fig, ax = plt.subplots(figsize=(15,9))

ax.grid(False)

X = np.arange(len(df.index))

ax.bar(X-0.2, df.year_1.values, width= 0.2, label='2017', color = 'g')
ax.bar(X, df.year_2.values, width = 0.2, label='2018', color = 'b')
ax.bar(X + 0.2, df.year_3.values, width = 0.2, label='2019', color = '#ff9900')

plt.gca().legend(loc='upper right', bbox_to_anchor=(1.13, 1.02))

ax.set_ylim([0, 100])
plt.xticks(X, df.index)
plt.xticks(rotation = 45)

ax.set_xlabel('Time (Months)', fontsize=16, fontweight="bold")
ax.set_ylabel('Percentage (%)', fontsize=16, fontweight="bold")
ax.set_title('Energy utilization', fontsize=18, fontweight="bold")

plt.savefig('energy_utilization.png', dpi=300)



df1 = pd.read_excel("waste.xlsx", sep=" ")

df1.columns = ['Time', 'year_1', 'year_2', 'year_3']

df1.set_index('Time', inplace=True)

sns.set_style("white")
sns.set(style="ticks", context="talk")

fig1, ax1 = plt.subplots(figsize=(15,9))

ax1.grid(False)

X1 = np.arange(len(df.index))
```

Appendix E

This script reads the production data which contains the monthly turbine energy, district heating energy, total energy produced, energy utilization and waste burn. The total energy produced, the turbine energy and the district heating energy data were selected and plotted as shown in Figure 18.

```
import pandas as pd
import datetime as dtm
from datetime import datetime, timedelta
import seaborn as sns
import time
import matplotlib.pyplot as plt
import matplotlib.dates as mdates

crt_yr = dtm.datetime.utcnow().year
crt_month = dtm.datetime.utcnow().month
crt_day =dtm.datetime.utcnow().day
crt_time = dtm.datetime.utcnow().replace(microsecond=0)
crt_hour = crt_time.hour
crt_minute = crt_time.minute
end_range = crt_time

start_time = dtm.datetime(year=2017, month=1, day=1, hour=0, minute=0)
end_time = dtm.datetime(year=2019, month=12, day=1, hour=0, minute=0)
start_time_2018 = dtm.datetime(year=2018, month=1, day=1, hour=0, minute=0)
end_time_2017 = dtm.datetime(year=2017, month=12, day=1, hour=0, minute=0)
end_time_2018 = dtm.datetime(year=2018, month=12, day=1, hour=0, minute=0)

df = pd.read_excel("Production_data.xlsx", sep=" ")
df = df.dropna()

df['Time'] = pd.to_datetime(df['Time'])
df.set_index('Time', inplace=True)

df['year'] = df.index.year
df['month'] = df.index.month
df['day'] = df.index.day

sns.set_style("white")
sns.set(style="ticks", context="talk")

fig, ax = plt.subplots(figsize=(20,11))

ax.plot(df.index, df.Energy_produced.values, label='Total energy produced', marker='o')
ax.plot(df.index, df.Energy_turbine.values, label='Energy turbine', marker='v')
ax.plot(df.index, df.Energy_district_heating.values, label='Energy district heating', marker='s')



plt.gca().legend(loc='upper right', bbox_to_anchor=(1.13, 1.012))

ax.xaxis.set_major_locator(mdates.AutoDateLocator())
plt.xticks(rotation = 45)

ax.set_ylim([0, 35000])
ax.set_xlim(left=start_time, right=end_time)
ax.xaxis.set_major_locator(mdates.MonthLocator(interval=2))
ax.xaxis.set_major_formatter(mdates.DateFormatter('%b-%y'))

ax.set_xlabel('Time(years)', fontsize=16, fontweight="bold")
ax.set_ylabel('Energy (MWh)', fontsize=16, fontweight="bold")
ax.set_title('Plant Thermal Energy', fontsize=18, fontweight="bold")

plt.savefig('combined_year.png', dpi=300)
```